

**A major purpose of the Technical Information Center is to provide the broadest dissemination possible of information contained in DOE's Research and Development Reports to business, industry, the academic community, and federal, state and local governments.**

**Although a small portion of this report is not reproducible, it is being made available to expedite the availability of information on the research discussed herein.**

**NOTICE**

**PORTIONS OF THIS REPORT ARE ILLEGIBLE. It has been reproduced from the best available copy to permit the broadest possible availability.**

LA-UR - 80-2271

**TITLE:** LECTURE 5: DISCHARGE CIRCUITS AND LOADS

**AUTHOR(S):** W. J. Sarjeant

LA-UR--80-2271

DE84 010044

**SUBMITTED TO:** University of New Mexico  
Graduate Course EECS596  
entitled  
"HIGH VOLTAGE/PULSE POWER TECHNOLOGY"  
  
and  
  
Los Alamos Scientific Laboratory  
E-Division Training Course  
entitled  
"POWER CONDITIONING TECHNOLOGY"  
  
(Course Coordinator: W. Sarjeant)

By acceptance of this article for publication, the publisher recognizes the Government's (license) rights in any copyright and the Government and its authorized representatives have unrestricted right to reproduce in whole or in part said article under any copyright secured by the publisher.

The Los Alamos Scientific Laboratory requests that the publisher identify this article as work performed under the auspices of the UHERDA.

This report was prepared as an account of work sponsored by an agency of the United States Government. Neither the United States Government nor any agency thereof, nor any of their employees, makes any warranty, express or implied, or assumes any legal liability or responsibility for the accuracy, completeness, or usefulness of any information, apparatus, product, or process disclosed, or represents that its use would not infringe privately owned rights. Reference herein to any specific commercial product, process, or service by trade name, trademark, manufacturer, or otherwise does not necessarily constitute or imply its endorsement, recommendation, or favoring by the United States Government or any agency thereof. The views and opinions of authors expressed herein do not necessarily state or reflect those of the United States Government or any agency thereof.

**DISCLAIMER**

**Los Alamos**  
**scientific laboratory**  
**of the University of California**  
LOS ALAMOS, NEW MEXICO 87544

An Affirmative Action/Equal Opportunity Employer

Form No. 816  
St. No. 2829  
1/74

UNITED STATES  
ENERGY RESEARCH AND  
DEVELOPMENT ADMINISTRATION  
CONTRACT W-7405-ENG. 38

**MASTER**

# HIGH VOLTAGE/PULSE POWER TECHNOLOGY

GRADUATE COURSE EECS596

University of New Mexico

## LECTURE INDEX

<u>Lecture</u>	<u>Lecture Topic</u>	<u>Instructor</u>
1	INTRODUCTION TO POWER CONDITIONING . . . . .	W. J. Sarjeant LASL
2	DC POWER SUPPLIES AND HARD-TUBE POWER . . . . . CONDITIONING SYSTEMS	W. J. Sarjeant LASL
3	PULSE VOLTAGE CIRCUITS . . . . .	W. L. Willis LASL
4	TRANSMISSION LINES AND CAPACITORS . . . . .	R. R. Butcher LASL
→ 5	DISCHARGE CIRCUITS AND LOADS . . . . .	W. J. Sarjeant LASL
6	SPARK GAPS . . . . .	W. L. Willis LASL
7	THYRATRONS AND IGNITRONS . . . . .	W. J. Sarjeant LASL
8	CHARGING SYSTEMS . . . . .	W. C. Nunnally LASL
9	PULSE TRANSFORMERS AND DIELECTRICS . . . . .	G. J. Rohwein Sandia Labs
10	MEASUREMENT TECHNIQUES . . . . .	W. L. Willis LASL
11	PARTICULAR APPLICATIONS . . . . .	R. R. Butcher LASL
12	E-BEAM SYSTEMS . . . . .	K. R. Prestwich Sandia Labs
13	GROUNDING AND SHIELDING TECHNIQUES . . . . .	T. R. Burkes Texas Tech U.

LECTURE 5  
DISCHARGE CIRCUITS AND LOADS  
by  
W. J. Sarjeant  
Los Alamos Scientific Laboratory

October 15, 1980

## PREFACE

With the recent increase in technological needs and the interest in the power conditioning arena, one of the problems facing workers in the field is the lack of texts or notes describing recent progress, particularly in the area of repetitive power conditioning. For this reason and because of expanding internal requirements, the University of New Mexico (UNM) and the Los Alamos Scientific Laboratory (LASL) have created a set of lecture notes based upon the graduate course taught recently at UNM. The objective of these notes is to create a record of many of the advances in the field since the last text in the field was published just after World War II. In this context, the lectures presented are oriented toward an introduction of the reader to each of the areas described and present sufficient background information to explain many of these advances. They are not intended to serve as design engineering notes, and thus the reader is referred to the references at the end of each lecture for detailed technical information in specific areas.

The preparation of these writings is a result of a considerable teamwork effort on the part of LASL and Sandia staff. In particular, Cathy Correll, in conjunction with Jo Ann Barnes and the rest of her efficient word processing staff, carried the major responsibility for preparation of the lectures while the lecturers did the proofreading and revisions. As course coordinator, it is a pleasure to acknowledge the strong support of Ray Gore, our E-Division Leader, and Shyam Gurbaxani who is the UNM Graduate Center Director, Los Alamos Campus.



W. J. Sarjeant  
Los Alamos Scientific Laboratory  
Los Alamos, New Mexico  
October 3, 1980

## LECTURE 5

	<u>Index</u>	<u>Page</u>
I.	INTRODUCTION . . . . .	1
	A. General Properties of the Discharge Circuit and Load . .	1
	B. Pulse-Forming Network Systems . . . . .	3
	C. Parasitic Capacitance Effects . . . . .	7
II.	THYRATRON, IGNITRON, THYRISTOR, AND THE LIKE . . . . .	7
	A. Switch Common Areas . . . . .	7
	B. Thyatron Switch Model . . . . .	7
III.	PULSE TRANSFORMERS . . . . .	9
	A. Pulse Transformer Models . . . . .	9
	B. Pulse Transformer Limitations . . . . .	12
IV.	SWITCH RECOVERY AND RESISTIVE EFFECTS . . . . .	14
V.	SWITCH RISETIME EFFECTS IN ULTRAFAST POWER CONDITIONING SYSTEMS . . . . .	16
	A. Switch Modeling . . . . .	16
	B. Trigger Generator for Multichannel Spark Gaps . . . . .	18
VI.	EFFECTS OF INTERCONNECTION PULSE CABLES TO LASER LOADS . . .	22
VII.	EFFECTS OF CHANGE IN THE LOAD IMPEDANCE ON CIRCUIT PERFORMANCE . . . . .	24
	A. Voltage Reversal After PFN Discharge . . . . .	24
	B. Voltage Reversal During Load Faults . . . . .	26
VIII.	EFFECT OF PARASITICS ON SYSTEM PERFORMANCE . . . . .	28

	<u>Index</u>	<u>Page</u>
IX.	PROTECTING THYRATRONS FROM EXCESSIVE VOLTAGES . . . . .	30
X.	EFFECTS OF LOAD SHORT CIRCUITS . . . . .	33
XI.	OPEN-CIRCUIT PROTECTION WITH CABLE INTERCONNECTIONS . . . . .	37
XII.	LASER LOADS . . . . .	37
	A. Direct-Discharge Pumped Excimer Laser Loads . . . . .	37
	B. Flashlamp Loads . . . . .	43
	C. Carbon Dioxide Laser Load . . . . .	47
	D. Discharge-Pumped Hydrogen Fluoride Laser Load . . . . .	49
XIII.	SUMMARY . . . . .	49
	REFERENCES . . . . .	53

## LECTURE 5

### INDEX TO FIGURES

<u>Figure</u>	<u>Title</u>	<u>Page</u>
1.	General properties of the discharge circuit and loads . . . .	2
2.	Impedance matching effects on the general properties of the discharge circuit . . . . .	4
3.	Pulse-forming network characteristics . . . . .	5
4.	Parasitic capacitances and their effects on pulse risetime . . . . .	8
5.	Thyratron switch model . . . . .	10
6.	Pulse transformer model . . . . .	11
7.	Pulse transformer limitations . . . . .	13
8.	Switch recovery and resistive effects upon circuit performance . . . . .	15
9.	Ultrahigh-speed spark gap trigger generator . . . . .	17
10.	HY-5301 thyratron model and trigger circuit initial conditions . . . . .	19
11.	Predicted trigger pulse shape using a HY-5301 thyratron switch . . . . .	20
12.	Predicted trigger pulse shape using a HY-5323 developmental thyratron switch . . . . .	21
13.	Effect of pulse cable between the fast-discharge circuit and a laser load . . . . .	23
14.	Effects of change in load impedance on the performance of line-type power conditioning systems . . . . .	25
15.	Further effects of change in load impedance on the performance of line-type power conditioning systems . . . .	27
16.	(a) Typical line-type PCS . . . . .	29
	(b) Waveforms showing load and thyratron current in a line-type power conditioning system with distributed capacitances . . . . .	29



<u>Figure</u>	<u>Title</u>	<u>Page</u>
17.	Inverse voltage removal during load faults . . . . .	31
18.	Inverse voltage calculation and removal during load faults .	32
19.	Load short-circuit faults . . . . .	34
20.	Inverse voltage appearing during load faults and nonlinear circuits to control this voltage . . . . .	35
21.	Open-circuit protection with cable interconnections . . . . .	38
22.	Circuit information for inductive loads . . . . .	39
23.	Simplified Excimer laser driver . . . . .	40
24.	Typical Excimer laser . . . . .	42
25.	Time history of circuit and system parameters in the discharge-pumped KrF* laser . . . . .	44
26.	Comparison of predicted and measured powers and impedances in the discharge-pumped KrF* laser . . . . .	45
27.	Flashlamp loads . . . . .	46
28.	Carbon dioxide laser loads . . . . .	48
29.	Discharge-pumped hydrogen fluoride laser load . . . . .	50
30.	Discharge-pumped hydrogen fluoride laser load, cont'd. . . .	51
31.	Apparent impedance of the discharge-pumped hydrogen fluoride laser load . . . . .	52

LECTURE 5  
DISCHARGE CIRCUITS AND LOADS

by  
W. J. Sarjeant

I. INTRODUCTION

This will be an overview in which some of the general properties of loads are examined:

- their interface with the energy storage and switching devices;
- general problems encountered with different types of loads;
- how load behavior and fault modes can impact on the design of a power conditioning system (PCS).

A. General Properties of the Discharge Circuit and Load

Consider, in Figs. 1 and 2, a transmission line with some impedance  $Z_0$  and a one-way transit time  $\delta$ , connected in series with an ideal switch, and a load resistor  $R_L$ . Now,  $V_0$  is the voltage to which the line is charged. When the ideal switch is closed, a current<sup>1</sup> equal to

$$\frac{V_0}{R_L + Z_0}$$

flows for a time  $\tau = 2\delta$ . For this discussion, let us accept this as an experimental fact. The pulse width  $\tau$ , base to base, is then  $2\delta$  for the case in which the load impedance equals the impedance of the transmission line.

For maximum energy transfer it can be shown that there is a relationship between the energy stored in the line and the energy delivered to the load. There is a broad maximum in the energy transfer efficiency (Fig. 1). Even with a significant impedance mismatch there can still be a quite high transfer of efficiency in the system. From 0.5 to 1.5 in the ratio of

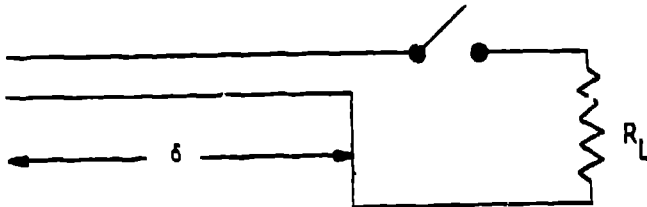
FIGURE 1: GENERAL PROPERTIES OF THE DISCHARGE CIRCUIT AND LOADS

General Properties:

- Basic characteristics determined by circuit elements: switch, PFN, and load.
- Pulse cable can introduce some pulse shape degradation, amplitude attenuation, and average power loss.

Ideal Discharging Circuit

Transmission Line:  
(impedance is  $Z_0$ )



$$i(t) = \frac{V_0}{R_L + Z_0} \quad 0 \leq t \leq 2\delta$$

$$= 0 \quad t > 2\delta \quad \text{if } R_L = Z_0$$

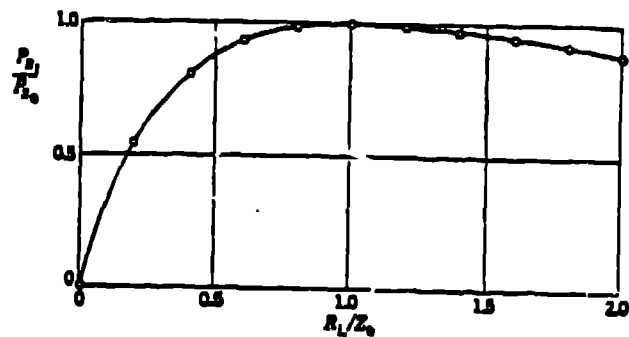
and  $2\delta \equiv \tau = \text{PULSE WIDTH}$   
where  $\delta$  is the one-way transient time.

For Maximum Energy Transfer,  $R_L = Z_0$ .

As  $R_L$  varies from  $Z_0$ :

$$P_{R_L} / P_{Z_0} = \frac{R_L}{Z_0} \cdot \left[ \frac{1}{(1 + R_L/Z_0)^2} \right]$$

$$P_{R_L} = \left[ \frac{V_0^2}{(R_L + Z_0)^2} \right] \cdot R_L$$



$R_L/Z_0$ , there is a transfer efficiency of about 80%. The real reason, in general terms, that the line impedance is matched to load impedance is to control the voltage left on the line at the end of the discharge cycle. If an 80 to 85% efficiency is acceptable, there can be a large mismatch.

When the load impedance equals  $Z_0$ , the impedance of the transmission line, the energy stored in the line is one-half  $C_0 V_0^2$  and it is all discharged into the resistive load  $R_L$  in the same time  $\tau$ . It can be shown (Fig. 2) that the energy deposited into the load is the integral of the instantaneous voltage times the current over the discharge time. The discharge time is twice the line capacitance times the line impedance. This is a useful relationship to keep in mind.

The pulse risetime problem in short-pulse duration discharge circuits is due to the parasitic capacitance across the load. The parasitic capacitance times the impedance of the transmission line gives a fairly good measure of what the ultimate risetime will be if the capacitance is fairly large. That is normally the property of the real-world system that degrades the voltage risetime on the load. The current risetime is determined primarily by the inductance in the switch-load interface area.

#### B. Pulse-Forming Network Systems

In the case of pulse-forming network (PFN) systems, Fig. 3 shows an example of a system having a unidirectional switch, a type E PFN (of four sections) discharging into an impedance equal to the PFN characteristic impedance. The PFN discharge current in each section is shown to illustrate the different current pulses flowing through the different capacitances in the line. The last capacitor in the line sees twice the peak current. The rms current through each is about the same, but the peak current in the final capacitor is definitely higher.<sup>1</sup> This means that

FIGURE 2: IMPEDANCE MATCHING EFFECTS ON THE GENERAL PROPERTIES OF THE DISCHARGE CIRCUIT

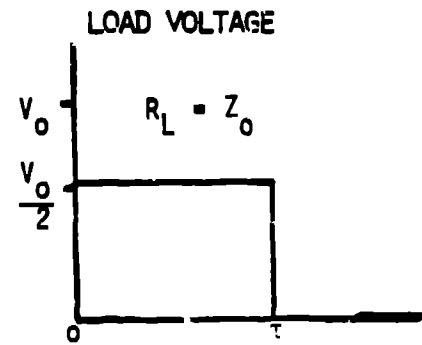
For  $Z_0 = R_L$ , all the energy in the transmission line is dissipated in  $R_L$ :

Let  $C_0$  = Line capacitance

$$\therefore \frac{1}{2} C_0 V_0^2 = \frac{V_0^2}{4Z_0} \tau = \frac{V_0}{2} I_0 \tau$$

$$\text{I.E.} = \frac{V_0}{2} I \tau = \frac{V_0}{2} \cdot \frac{V_0}{2Z_0} \tau = \frac{V_0^2}{4Z_0} \tau$$

$$\text{or } \tau = 2C_0 Z_0 = \text{Pulse duration}$$



Note that stray capacitances may degrade very short pulse length pulse shapes.

## FIGURE 3: PULSE-FORMING NETWORK CHARACTERISTICS

PFN:

Very fast risetimes and falltimes demand tapered PFNs. Low ripple demands many sections.

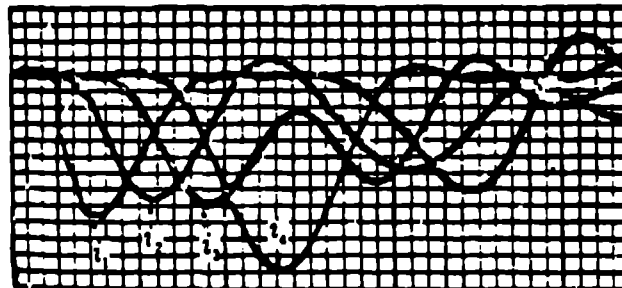


Fig. 6-40.—Condenser-discharge currents in the four-section type-E network shown in Fig. 6-40.

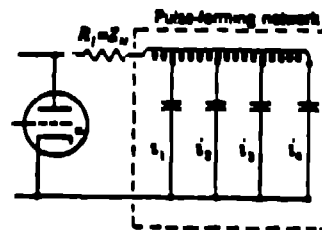


FIG. 6-40.—Circuit diagram for Fig. 6-39.

Ref. 1

during the design of a PFN it is usually more cost-effective to provide the capacitor supplier with a sketch of the network along with the capacitor values and inform him of the load peak current, allowing him to design the capacitors for this service taking into account the current ratios in the various PFN capacitors.

For very short-duration current pulses in the multikiloamp range, the PFN capacitor is preferably of the extended-foil type to eliminate internal arcing and tab interface power losses.<sup>2</sup> If the current risetime required in the load is less than  $0.1 \tau$ , there is a way of achieving this, which was started years ago in gas discharge systems. Given an ideal switch in a four- to eight-section transmission line, the first four capacitances are selected in the ratio of 1:2:4:8 and the same impedance per section,  $Z_0 = \sqrt{L_N C_N}$ . This does not produce a trapezoidal shaped pulse, but it gives a very fast risetime pulse. In this configuration, water vapor lasers were driven with relatively steep rising current pulses. Because they were direct electron-pumped systems, this increased the electron temperature significantly and increased their laser efficiency. The risetime is effectively the discharge time for the very first stage provided the PFN-load interface inductance  $L$  is small enough so that  $L/R_L$  is less than the first PFN section discharge time. This is generally a useful technique for generating a steep wave-front pulse. Time-varying load impedances can be roughly matched for these lasers by setting a ratio for the impedances of  $Z_0$  to 2:4:8 for the first three sections, creating what is called a tapered transmission line. This can cause reflection problems, but it is a rather unique and efficient way of driving such loads as hydrogen fluoride (HF) lasers,  $\text{CO}_2$  transversely KrF Excimer systems, whose impedance decreases with time. This is a crude but economical approximation to the general time-varying PFN problem.

For very low ripple on the top of the pulse, there must be many sections in the PFN. A 20-section PFN can be built to have a peak-to-peak ripple of one per cent, which appears to be a practical limit. It is very difficult to achieve less ripple than this.

### C. Parasitic Capacitance Effects

A major problem in all these system can be parasitic capacitance and its effects on risetime (Fig. 4). In most cases two of these parasitics predominate: there is one across the switch and there is another across the load. Both are difficult to avoid. The one across the switch is discharged at an extremely high frequency when the switch closes. This could be used to advantage in spark gaps to shorten the resistive phase. The one across the load slows the rate of rise of voltage, creating problems in very fast circuits.

## II. THYRATRONS, IGNITRONS, THYRISTORS, AND THE LIKE

### A. Switch Common Areas

This section also discusses thyratrons, ignitrons, thyristors (silicon-controlled rectifiers), or any bulk ionization device where everything is controlled by avalanche ionization and the appropriate analogue in the solid-state case. EG&G has been studying thyratrons for the Los Alamos Scientific Laboratory AP Division to determine the limitations in their switching properties, the maximum speed at which they can be made to switch, and the physical model that correlates with the real world. It turns out that they can be made very fast switches indeed. Ristic shows that in spark gaps,<sup>3</sup> for the case of nitrogen, the gap voltage decreases with time and Ristic found a  $t^{-3}$  dependence. There is a great deal of discussion about this time dependence and the reader is referred to Lecture 6 on Spark Gaps for additional information.<sup>4</sup>

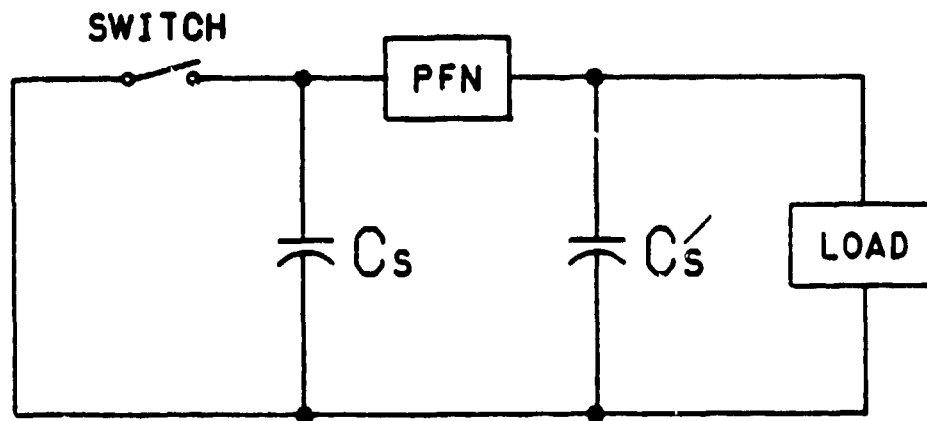
### B. Thyatron Switch Model

For thyratrons, a trigger pulse is applied, there is then an avalanche growth of electron density forming a glow discharge that may tend towards an abnormal glow for high peak currents. All switches of this class work this way. At  $t = 0$ ,  $-V_0$  is added in series with the switch so that no current flows. As time passes, the voltage source decreases in



FIGURE 4: PARASITIC CAPACITANCES AND THEIR EFFECTS ON PULSE RISETIME

For most applications, stray capacitances in the power conditioning system fast discharge portion can be lumped into a " $C_s$ " at the output of the PFN.



$$\tau_r = Z_{\text{PFN}} \cdot C_s'$$

amplitude and current flows through the system. The current flow is limited in its risetime by the lumped inductance  $L$ , which couples the switch and the load. The voltage drop decreases exponentially to the constant switch drop level for the duration of the pulse. The best values experimentally achieved for  $\tau_F$  are 1 ns for thyratrons at kiloamp peak current. That is a factor of 10 better than the initial value some 20 years ago.<sup>1</sup>

For thyratrons, the model that gives very good results in comparison to the data, with the discharge times of 20 to 100 ns, replaces the thyatron with a voltage source (Fig. 5). When the switch is closed, it has a series inductance (from the thyatron and its connections), a voltage source in series with it, plus the switch drop (which is an invariant 100 to 200 V for almost all gas switches). The  $\tau$  that gives the best agreement with the data is, if  $\tau_F$  is the total falltime from top to bottom,  $3\tau = \tau_F$ . That gives agreement, within 5 to 10%, with the data for all types of tubes. The examples we shall show later using this model predict somewhat slower rates of rise than are observed with present thyatron switch tubes.

### III. PULSE TRANSFORMERS

#### A. Pulse Transformer Models

Pulse transformers (Fig. 6), referring everything to the secondary, have a magnetizing inductance  $L_E'$ , a shunt capacitance  $C_C$ , primary to ground converted to secondary, the secondary-to-ground capacitance  $C_D$ , the leakage inductance  $L_L$ , the core loss  $R_E'$ , the load resistance  $R_L$ , and the voltage,  $NV_0$ . The switch, actually on the primary, is closed with everything referred to the secondary. The diagram then shows an LRC circuit with the risetime  $L_L$ - $C_D$  limited.

FIGURE 5: THYRATRON SWITCH MODEL

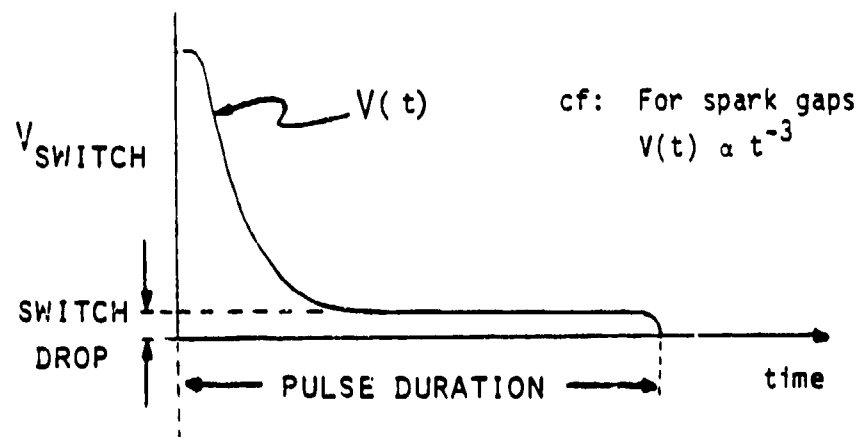
Most Current Model:

Let  $V(t)$  be the voltage across the switch,

Then:

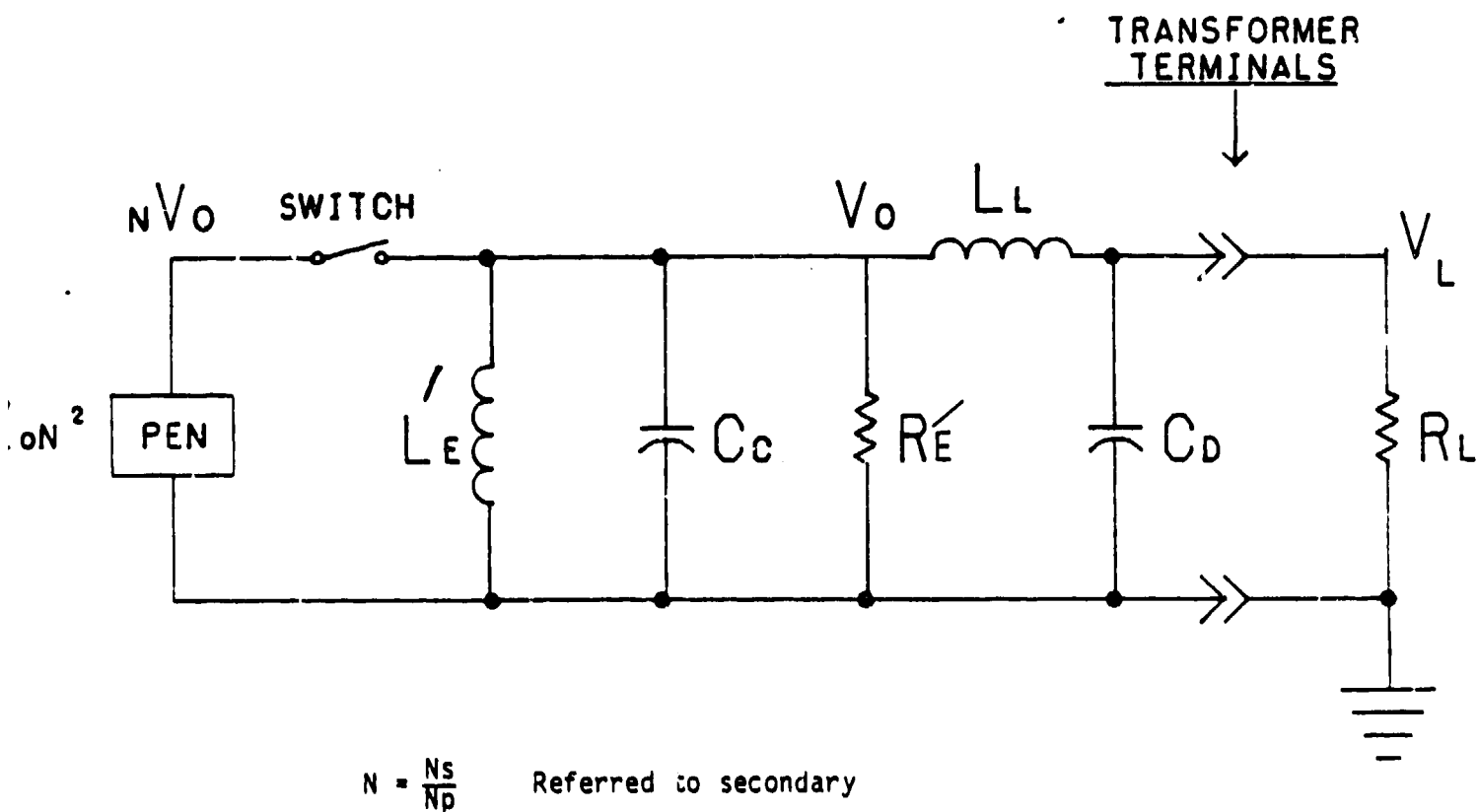
$$V(t) = V_0 (+e^{-t/\tau}) + \text{switch drop of } \approx 150 \text{ volts}$$

$3\tau = \tau_F = \text{Resistive phase falltime (i.e., 100 to 0\% voltage falltime)}$



Note: That for most switches the drop is nearly independent of current.

FIGURE 6: PULSE TRANSFORMER MODEL.



$L'_E$ : Magnetizing inductance  $\approx L_E N^2$

$R'_E$ : Core loss  $\approx N^2 R_E$

$L_L$ : Leakage inductance  $= L_L^{sec} + N^2 L_L^{pri}$

$C_D$ : Shunt capacitance-secondary to ground

$C_C$ : Shunt capacitance-primary to ground  $= C_p / N^2$

High-pulse fidelity pulse-transformer design is still a compromise of efficiency against pulse fidelity (Fig. 7). Flatness is predominantly controlled by three factors: resonances in the transformer structure, flux saturation level and the time taken to reach saturation (which is material dependent), and the amount of energy that flows into the magnetizing inductance. For very long pulses, it is the magnetizing inductance that shunts away the desired energy from the PFN. The cost of large, high-quality

pulse transformers goes up very rapidly with pulse width. Unless absolutely necessary, pulse transformers are an expensive route for pulses longer than 20 to 25  $\mu$ s.

### B. Pulse Transformer Limitations

Given a load like a magnetron or a direct-discharge-pumped gas laser, as the current and the voltage start to decrease, the sustaining voltage is passed and the current suddenly ceases to flow in the load, except for the current flow in the recharging inductance or resistance across the load. The falltime limit is then determined by the total loop inductance  $L$ , which for pulse transformer drive can easily be 400 to 500 nH, and the PFN impedance, resulting in fairly long falltimes. When a laser switches off, the energy stored in this shunt inductance and in the transformer leakage inductance discharges in a resonant fashion into the inductance/capacitance loop (Fig. 7). Another problem is that since this is a resonant discharge there can be a voltage reversal at the load point. The amount can be determined through a nonlinear analysis for high-power pulse transformers, but it is difficult to do. The amount of reversal is not constant as the load impedance changes. The load and the pulse transformer are intimately interconnected.<sup>1</sup>

For very fast pulses, coaxial cable transformers can be used to provide voltage gains of two to four times, but they are always rather high impedance. Cable transformers experimentally give much lower multiplications

## FIGURE 7: PULSE TRANSFORMER LIMITATIONS

Main problem areas are:

1.  $\tau_R \approx \pi \sqrt{L_L C_D}$  : Risetime limit
2. Flatness - determined primarily by resonances in  $L_L C_D$ ,  
and flux "saturation" level and time, and energy in  $L'_E$ .
3.  $\tau_F \approx \pi \sqrt{(L'_E + L_L) C_D}$  : Falltime limit - especially  
if  $R_L$  is biased diode load.  
  
 $\approx \pi \sqrt{L'_E C_D}$   
 since  $L'_E \gg L_L$  in general
4. Reversal depends upon matching and Q of circuit.

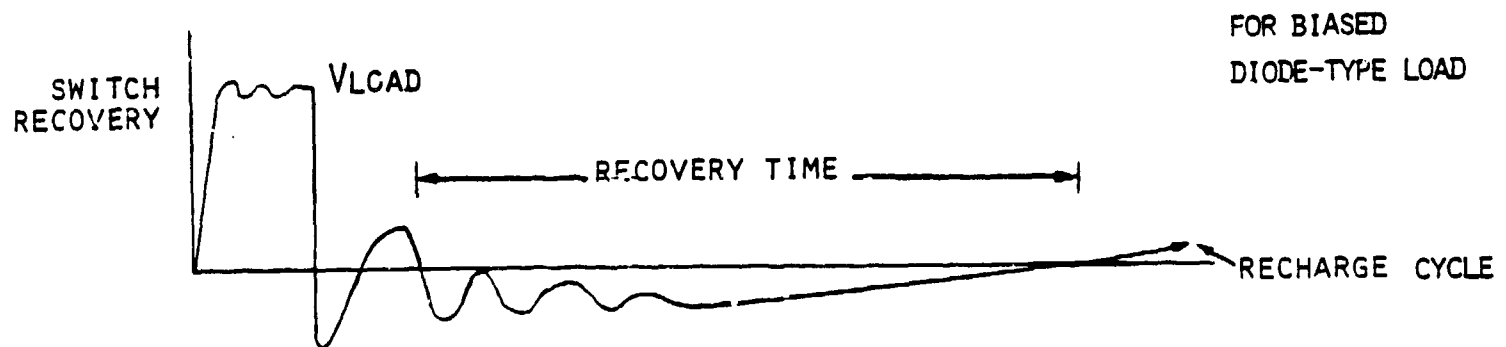
than the theoretical formula predicts. For two or three times, they are an economical way of stepping up voltages. All comments made for the same transformer using ferrite cores to increase permeability also apply to these.

For overall pulser efficiencies, a rough number is about 60 to 80%, which has not changed significantly since the 1940s. A repetition-rate system, even at 1 to 2 kHz has a given input power of about 70% of a given output power for the system. This is due to heat lost in the diodes and driving unit, and switch losses. This applies to ignitrons, thyratrons, vacuum arc devices, and some thyristor (silicon-controlled rectifier) modulators. Spark gaps in repetitive circuits can have quite large losses, and overall system efficiencies can fall well below 60% at kilohertz repetition rates.<sup>4</sup>

#### IV. SWITCH RECOVERY AND RESISTIVE EFFECTS

When a load turns off, the current decays towards zero. The resonance effect in all the inductors with the stray capacitances and the recharge circuit tries to put charge back on the PFN. The recovery time for the switch device, whatever it is, is over the time so marked in Fig. 8. The area of the first negative pulse represents a positive ion energy deposited inside the thyatron gas switch tube ("gas cleanup"), which can, in effect, increase the heat load on the tube and severely limit the lifetime.<sup>1</sup> In large, high-repetition-rate systems, where the switch tube is being pushed to the limit of its performance, an enormous amount of positive ion heating of the anode of the tube can occur, easily equaling the anode heating of the tube during the switch turn-on time. A similar behavior can apply to spark gaps. Energy is deposited in several areas inside the gap until it fully recovers. Just how important that is depends on the individual circuit.

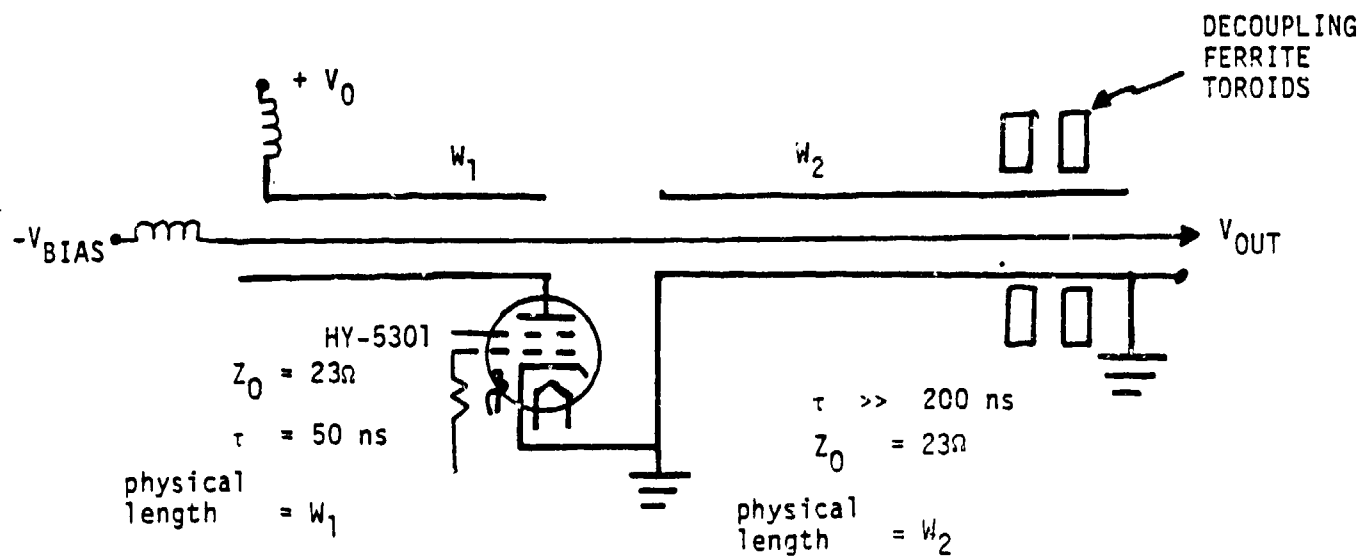
FIGURE 8: SWITCH RECOVERY AND RESISTIVE EFFECTS UPON CIRCUIT PERFORMANCE

Effect of Switch Resistance:

→ Primarily degrades risetime of voltage pulse



FIGURE 9: ULTRAHIGH-SPEED SPARK GAP TRIGGER GENERATOR



$V_{out}$  as a function of time, using NET 2 program and thyatron model as shown in Fig. 5:

For thyatron:

Tube drop = 150 V

$\tau_F = 10 \text{ ns} \therefore \tau = 3.3 \text{ ns} = 1/3 \cdot \tau_F$

and  $L = 20 \text{ nH} = \text{tube plus mounting inductance}$

Ref. 5

## V. SWITCH RISETIME EFFECTS IN ULTRAFAST POWER CONDITIONING SYSTEMS

The switch can degrade the risetime. This is illustrated by considering a circuit in Fig. 9 proposed for a mid-plane spark-gap trigger.<sup>5</sup> It is necessary to put a negative bias on the midplane through a coaxial cable. The inductor to the bias line decouples the midplane during the trigger pulse duration. The line of length  $W_1$  is resonantly charged to voltage  $V_0$ . The switch is closed, which then discharges this line into the second one of length  $W_2$ . There is a negative-going pulse on the second line, and the peak value equals the bias voltage plus the absolute value of  $V_0$ . The particular circuit under consideration has a 23- $\Omega$  line, 50 ns long, charging another 23- $\Omega$  line. The second line, being a long cable, eliminates reflections during the spark gap turn-on phase. The ground current through the coaxial outer conductor is decoupled with ferrite toroids that have been shown to work very well. There are several ferrite toroids that work particularly well for fast-pulse circuitry (e.g., Ferroxcube type 144T50G). About 20 to 30, spaced along the line, will provide a great deal of increased shield inductance. They increase the effective inductance between the grounds shown to minimize current flow through the cable during discharge.

A. Switch Modeling

Bill Nunnally has modeled this with a switch-resistive phase time,  $\tau_F$ , of 10 ns, a  $\tau$  of 3.3 ns, and a lumped switch plus interconnection inductance of 20 nH.<sup>5</sup> This is comparable to state-of-the-art systems. (Such a thyatron switch tube is about 1 in. high, and with a current return shroud attached, a total inductance of 10 to 15 nH is measured.) For an ordinary thyatron of conventional design, which is much larger in size, the inductance can be 200 to 300 nH. In the thyatron trigger, for conventional tetrode tubes,  $\tau_F$  is  $\approx$  40 ns and 80 ns for triodes. The tube model is illustrated in Fig. 10.

Initially the thyatron is at +50 kV and the bias on the spark gap at -50 kV. A 50-pF shunt load is assumed across the end of that line. The 23- and 50- $\Omega$  cables were selected and were found to have little effect on rise-time. The switch is a HY-5301, and gives an output pulse (Fig. 11) rate of rise of 7.5 kV/ns, which is more than adequate for multichanneling most spark gaps that require 6 kV/ns. An ordinary thyatron provides only 1.5 to 2 kV/ns. This is, then, a relatively compact switch device that can be used to provide fast trigger systems.

#### B. Trigger Generator for Multichannel Spark Gaps

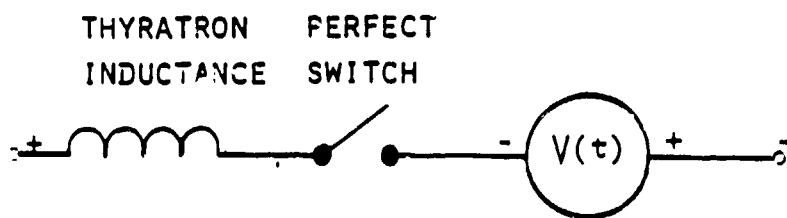
Another tube examined was a developmental 100-kV device (HY-5323), with a 15-ns resistive phase falltime and 30-nH total inductance. The advantage of going to the higher voltage is the steeper slope (Fig. 12). For multichanneling, the calculated 11 kV/ns is more than adequate. This pulse can be generated at repetition rates of several kilohertz with low delay times and extremely low jitter.

FIGURE 10: HY-5301 THYRATRON MODEL AND TRIGGER CIRCUIT INITIAL CONDITIONS

System Initial Conditions

$V_{bias} = -50 \text{ kV}$   
 $V_o = +50 \text{ kV}$   
 $C_L = 1 \text{ pf and } 50 \text{ pf: Load shunt capacitance}$

Use thyatron model: For HY-5301 tube



$$V(t) = -(50,000) e^{-(t-t_0)/\tau_R} + 150$$

Tube Drop  
when fully  
conducting

$V_o = 50,000 = \text{peak voltage across tube}$

$20 \text{ nH} = \text{tube inductance}$

$t_0 = \text{time at which perfect switch is instantly closed}$

$\tau_F = \text{resistive phase time for thyatron}$

$\approx 10 \text{ ns}$

Note: For conventional tubes

$\approx 3\tau$

$\tau_F \approx 40 \text{ ns}$  resulting in some  
risetime degradation time

where:  $\tau$  is  $1/e$  time

Ref. 5

FIGURE 11: PREDICTED TRIGGER PULSE SHAPE USING A HY-5301 THYRATRON SWITCH

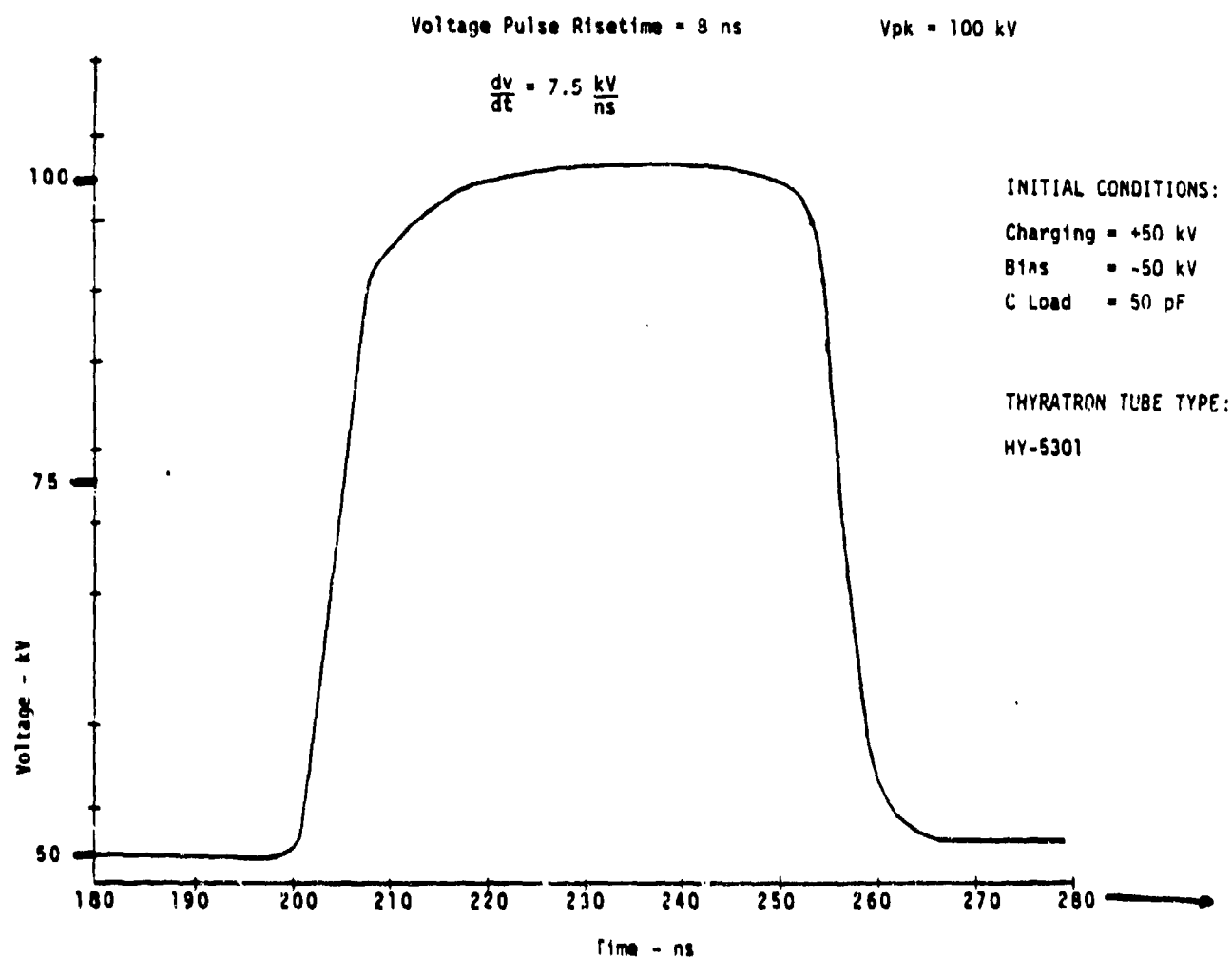
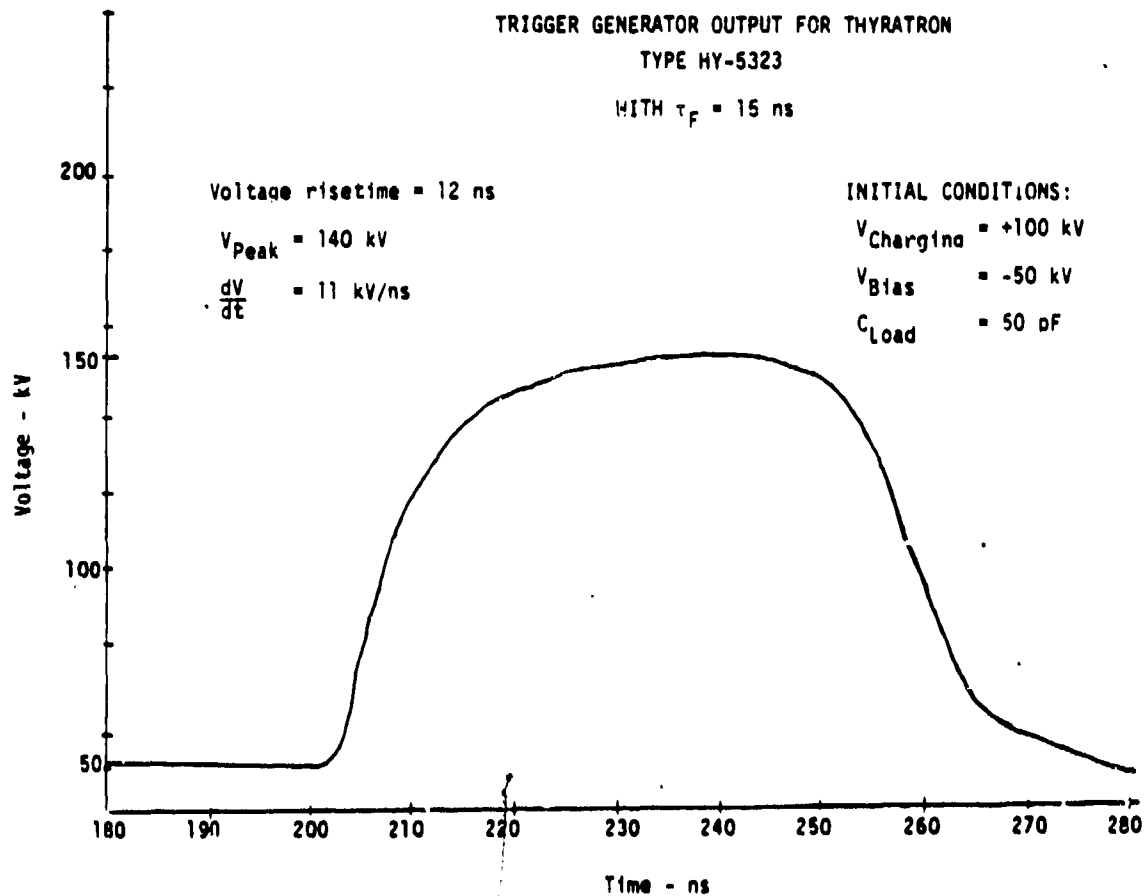


FIGURE 12: PREDICTED TRIGGER PULSE SHAPE USING A HY-5323 DEVELOPMENTAL THYRATRON SWITCH



Ref. 5

## VI. EFFECTS OF INTERCONNECTION PULSE CABLES TO LASER LOADS

There are four points to note on the effects of pulse cables connecting to laser loads (Fig. 13).

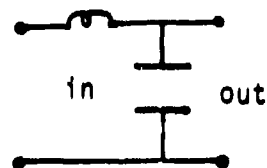
1. Given a piece of cable connecting the laser to the pulser, the laser impedance being usually time-varying, reflections can travel back and forth on the cable, causing oscillations on top of the voltage pulse.
2. Coaxial cables are not perfect cables; they have leakage inductances of about 15% and resistive losses. To derive the same peak power from the system, additional power must be put in the input. To minimize this, special totally shielded cable can be purchased, or high-voltage coaxial cable for underground power distribution systems is readily available at less cost and generally works well.
3. When the load faults, an opposite polarity voltage pulse travels back along the cable. Depending on the timing of the fault, enormous voltages can accumulate at the input of the cable. This problem is discussed in detail in Greenwood,<sup>6</sup> Ch. 3. Generally, if the cable is designed to handle three times the pulse load voltage, faults will not destroy the system. Most faults will not exceed three times the load voltage.
4. For fast pulses of about 1-ns risetime, there is very little current penetration into the conductors. The voltage pulse shape rapidly degrades substantially as it travels down the cable. The skin effect is well discussed in the book by Metzger and Varbre.<sup>7</sup> The problem was minimized in one case by keeping the cables shorter than 20 ft for 6-kV, 120-ps pulses. One-nanosecond pulses can be propagated for 100 ft over RG-17 and -19 uncompensated cables, if the cable is kept free of disturbances and physical damage. The fork lift degradation factor is 0.1 and 5%, reflection added per run-over. Foam cables are quite good, but should be strung overhead to avoid physical damage. (RG-8 foam will operate to 6-kV pulse at low-repetition rates.)

FIGURE 13: EFFECT OF PULSE CABLE BETWEEN THE FAST-DISCHARGE CIRCUIT AND A LASER LOAD

For laser loads, pulse cables create:

1. Reflection oscillations on pulse crest
2. Current increases because of cable resistive losses and radiation (shields not perfect).
3. For load faults, cable can propagate more than  $2V_0$  reflections depending upon total circuit Q.
4. For fast pulses ( $\approx$  nanosecond risetime) skin effect degrades risetime over  $\approx 30$  m for RG-17U.

Note that the cable looks like:



for pulse durations much longer than its two-way transit time. Then this cable acts as a resonant circuit in conjunction with PFN and/or transformer stray C and L. This can give rise to post-discharge oscillations that may be damaging to the switch or load. Damping shunt L-R networks in series with the coaxial cable center conductor at both ends of the cable generally control this.



In times much longer than the two-way transit time of the cable, a resonant circuit with a series L and a shunt C develops. Pulse discharge oscillations can be dampened in many cases by adding L/R networks in series with the center conductors at both ends of the cable, as will be discussed in detail somewhat later on.

## VII. EFFECTS OF CHANGE IN THE LOAD IMPEDANCE ON CIRCUIT PERFORMANCE

Difficulties arise with a time-varying load or one that can have pulse-to-pulse fluctuations (Fig. 14). The TEA CO<sub>2</sub> and the H<sub>2</sub> lasers have built-in fluctuations that are not necessarily repeatable or constant, while vacuum devices like magnetrons and klystrons have almost perfect reproduceability. Many of the fluctuations are caused when the loads arc, posing the problem of protecting the PCS from serious damage.

### A. Voltage Reversal After PFN Discharge

An ideal switch discharging a PFN has a charge voltage  $V_N$ , a current through the load, a voltage across the load, an impedance  $Z_N$  (of the PFN) and a load resistance  $R_L$  on the output. At the end of the discharge time, a voltage can be left on the line. The amount of reversal is<sup>1</sup>

$$\frac{V_{N-1}}{V_N} = \frac{R_L - Z_N}{R_L + Z_N}$$

where  $V_{N-1}$  is the peak voltage of the first reversal.

When  $R_L$  is smaller than  $Z_N$ , which is unfortunately the case for most lasers, there can be a significant degree of voltage reversal. With a unidirectional switch, the charging circuit gradually puts current into the PFN and starts recharging. Fundamentally, this negative voltage must be kept within the inverse ratings of the switch device. A typical number for ignitrons is 15 kV, for newer thyratrons 15 to 20 kV, and for older

FIGURE 14: EFFECTS OF CHANGE IN LOAD IMPEDANCE ON THE PERFORMANCE OF LINE-TYPE POWER CONDITIONING SYSTEMS

For rapid impedance changes during a pulse or pulse-to-pulse variation, usually caused by load faults, the designer must protect pulser against prolonged short or open circuits in the load loop.

FOR IDEAL PULSER DISCHARGING A PFN OF IMPEDANCE

$Z_N$  INTO RESISTIVE LOAD  $R_L$ :

$$I_L = \frac{V_N}{R_L + Z_N} \quad V_N = \text{PFN charge voltage}$$

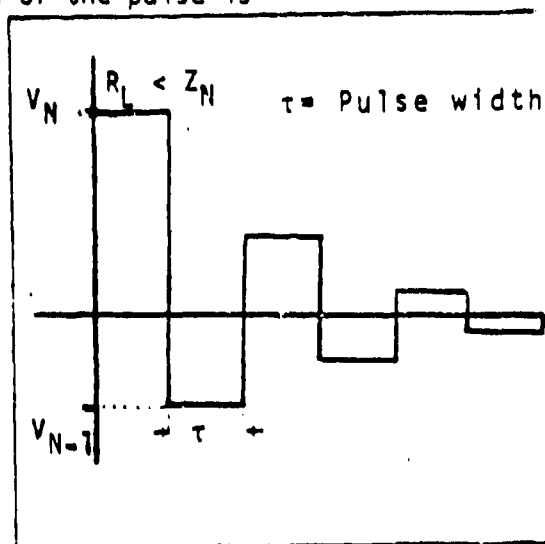
$$V_L = \frac{V_N}{R_L + Z_N} \times R_L$$

Voltage left on the network at the end of the pulse is<sup>1</sup>

$$V_{N-1} = \frac{R_L - Z_N}{R_L + Z_N} \times V_N$$

$\therefore$  % Voltage Reversal on PFN  
For BIDIRECTIONAL SWITCH:

$$100 \times \frac{V_N - V_{N-1}}{V_N} = \frac{2Z_N}{R_L + Z_N}$$



NOTE: For biased diode load, if  $V_{N-1} < V_{\text{threshold}}$  of the load then discharge is through recharge elements in parallel with the load.

Ref. 1

thyratrons 5 kV. If this number is exceeded the device arcs. Arc damage depends solely upon the properties of the switch tube. Ignitrons, even at high-repetition rates, can handle some intermittent arcing. Thyratrons usually include protective snubber devices to keep the voltage under control. If the load does arc and it is a tetrode thyatron tube, basically nothing happens to it because there is the forward bias plasma in the cathode region, and thus when the switch breaks down from excessive inverse voltage, it tends to do so in a bulk ionization mode. Spark gaps of course are fully bidirectional and thus can handle inverse currents with no problem.

If the inverse voltage is less than whatever is needed to turn the load back on in the reverse bias direction, the PFN discharges through the shunt element that is in parallel with the load, which is either the inductor or resistor used to allow the PFN to recharge. The negative voltage just discharges through those elements.

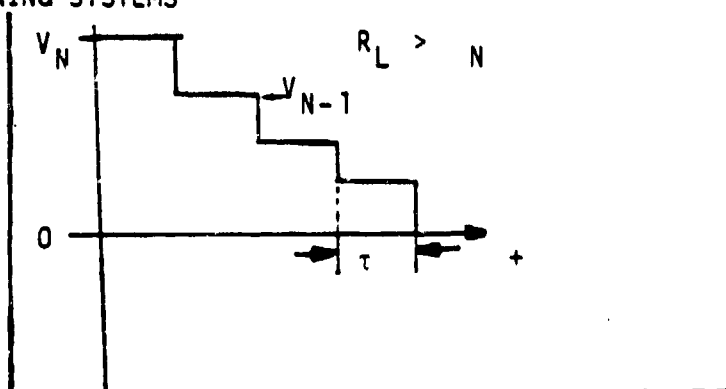
When the load resistance is greater than  $Z_N$ , a step results (Fig. 15). When lasers or magnetrons turn off, the impedance becomes very large and a long time to zero can follow. Spark gaps and ignitrons have no problem handling this, but thyratrons do. Older modulators were designed using this positive mismatch to avoid inverse voltage on tubes. It was felt that there must always be a time at which the voltage and current must reach zero to let the tube recover. Today, the best way to achieve this goal is to pulse charge the PFN. Instead of only a resonant or resistive charging unit, a switch is put in series with them and turned on to recharge the PFN well after the output switch has recovered.

#### B. Voltage Reversal During Load Faults

If there is a short-circuit fault in the load during the discharge, it almost instantaneously puts  $-V_N$  across the PFN. If the switch recovers,

FIGURE 15: FURTHER EFFECTS OF CHANGE IN LOAD IMPEDANCE ON THE PERFORMANCE OF LINE-TYPE POWER CONDITIONING SYSTEMS

NOTE:  $R_L < Z_N$  case with unidirectional switch: switch opens when voltage across it passes through zero. Then PFN has  $V_{N-1}$  on it at beginning of next charge cycle. For example, in resonant charging:



$$V_{Nth} \text{ charging period} = V_{DC} + (V_{DC} - V_{J_{N-1}}) e^{-R_c T_r / 2L_c}$$

$V_{J_{N-1}}$  = voltage left on PFN after N-1 discharge

$$T_r = \pi \sqrt{L_c C_{PFN}}$$

$L_c$  = Charge L  
 $R_c$  = Loss resistance  
 in L

For example, let the load fault with unidirectional switch leaving  $-V_N$  upon PFN

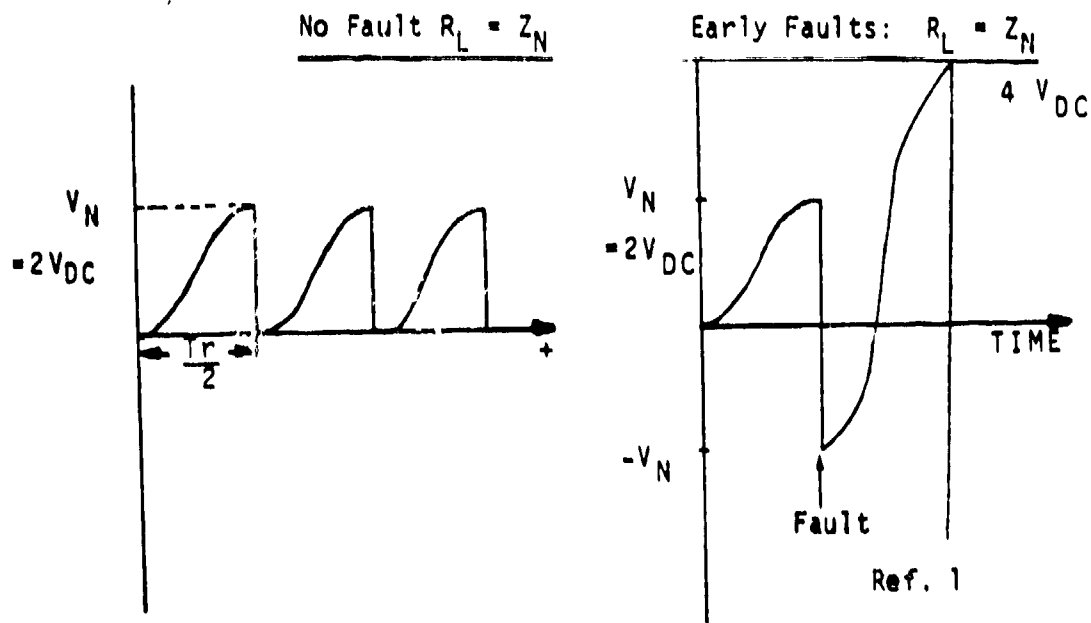
$$\therefore V_1 = V_{DC} + (V_{DC} + V_N) e^{-\pi/2Q} \text{ and } V_N = 2V_{DC}$$

$$\text{If } Q > 10 \therefore e^{-\pi/2Q} \approx 1$$

$$\therefore V_1 = V_{DC} + (V_{DC} + 2V_{DC}) = 4V_{DC} \gg V_N$$

GENERALLY SWITCH FAULTS AND PULSER OVERVOLTAGE/CURRENT SENSORS TURN HV OFF

Cases of interest for PFN charging voltages:



it starts charging from  $-V_N$  and resonantly charges up to four times the peak dc (Fig. 15). A general property of resonant circuits<sup>1</sup> is that they will charge up to twice the sum of the absolute value of the voltage below the zero line plus the dc voltage. At high voltages, the switch tube faults as it exceeds its forward hold-off voltage, and the protection circuits in the system must come into play.

#### VIII. EFFECT OF PARASITICS ON SYSTEM PERFORMANCE

A sketch of a typical line-type PCS is given in Fig. 16(a), with several stray capacitances shown. The inverse diode  $D_2$  is used to clamp any negative voltage left on the PFN at the end of the discharge cycle or during load faults. The charging diode is  $D_1$ . The World War II modulator designs used the vacuum diodes shown, which could be replaced with solid-state diodes. There are still, however, stray capacitances. When the switch tube is turned on,  $C_s$  and  $C_s'$  contain stored energy, and being small, force the tube to shunt to ground this energy at a very high rate of rise of current and oscillations occur. In system design, a current-viewing resistor (e.g., T&M, Inc., Type W) should always be inserted in the circuit in the cathode of the thyatron, ignitron, krytron, etc. (Current transformers are difficult to use in very fast circuits: they have a non-Gaussian response and give rise to shock-excited oscillations with a driving current waveform that has a front risetime faster than their effective risetime.) If oscillations are apparent, the lifetime of the device in the PCS usually will be shortened. During the rapid time-varying resistive turn-on phase, the instantaneous power dissipated in the device can be excessive.

Oscillations can be dampened with a shunt LR network in the thyatron anode lead. Choose a Q less than 2 if possible. Ohmite makes a parasitic suppressor used for suppressor grid and neutralization oscillation suppression. It is a 50- $\Omega$  resistor in parallel with a silver-plated inductor of 0.3- $\mu$ H inductance and is inexpensive. They can be used in series with the anode of the tube and are effective.

**FIGURE 16(a): TYPICAL LINE-TYPE PCS**

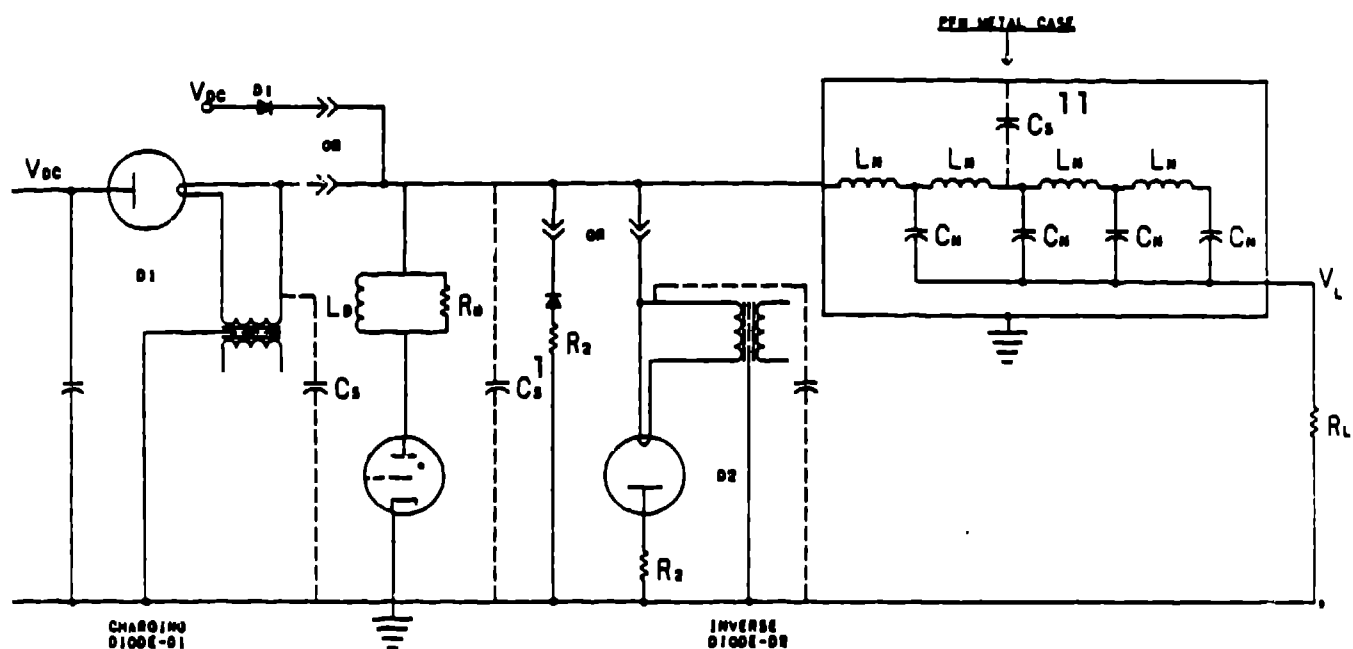
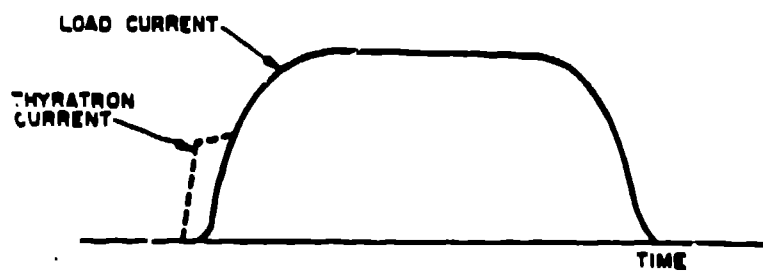
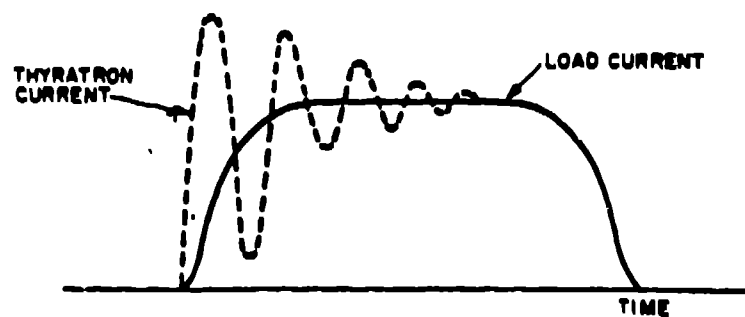


FIGURE 16(b): WAVEFORMS SHOWING LOAD AND THYRATRON CURRENT IN A LINE-TYPE POWER CONDITIONING SYSTEM WITH DISTRIBUTED CAPACITANCES



(a)



(b)

**Ref. 8**

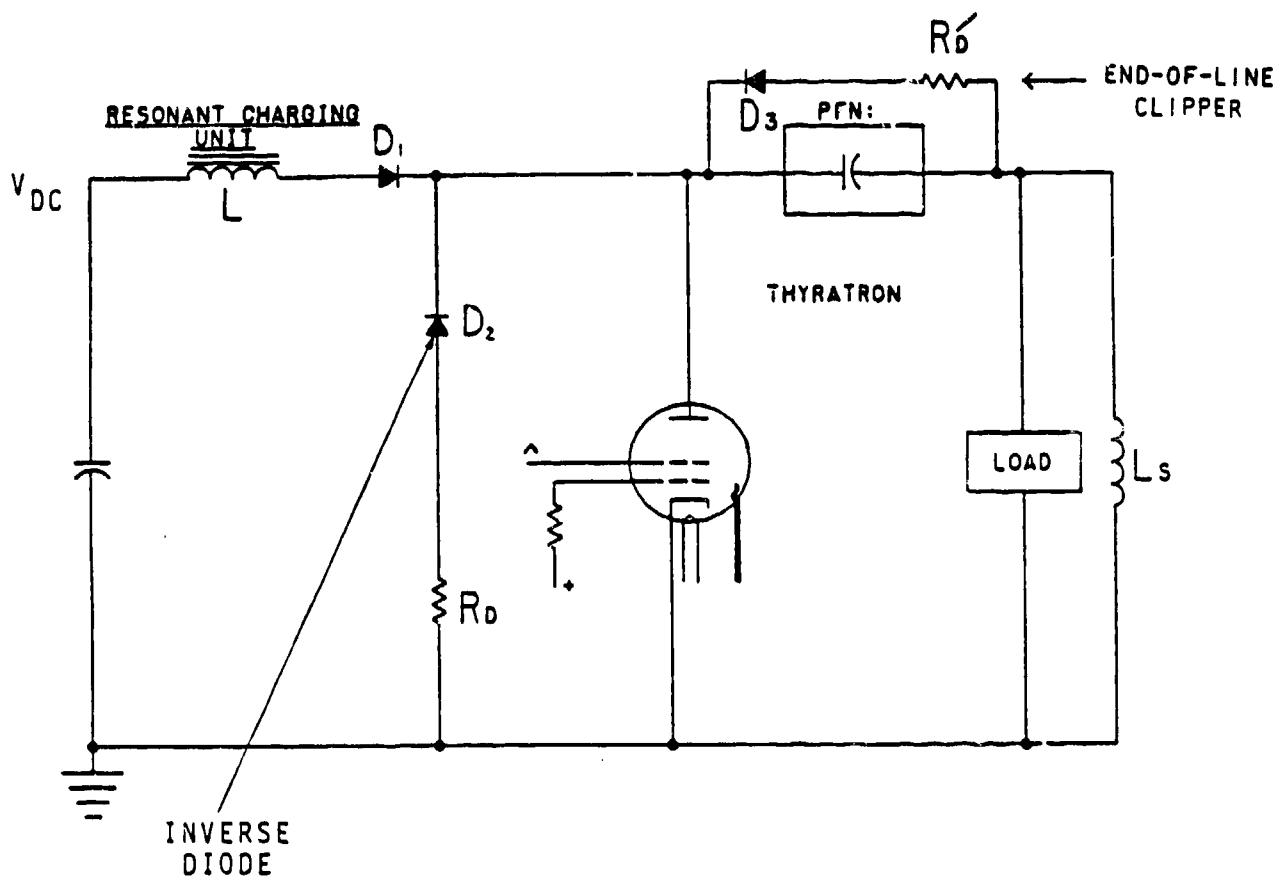
Spark gaps also dissipate power during the turn-on time. That is a waste of the capabilities of the device, and the losses should be minimized by reducing the turn-on time.

#### IX. PROTECTING THYRATRONS FROM EXCESSIVE VOLTAGES

If there is a short on the load (Figs. 17 and 18) and if a resistor equal to the impedance of the load could be instantaneously put in parallel with the switch tube, the maximum apparent voltage would be  $-V_{dc}$ . With a noninductive resistor inserted in the circuit during a short, a tube charged to +50 kV will see -25 kV on the anode and the tube could arc back. With a tetrode tube, the arc damage from occasional faults is not significant. To really protect the tube a shunt network could be added from anode to ground. Adding a diode-resistor end-of-line clipper across the PFN ( $R_D' = Z_0$ ), then 12.5 kV will result and the tube will be safe.<sup>1</sup> The biggest problem is the turn-on time of the diode. Many diodes have fast turn-on times, but are capacitively graded and have very little protection from stray electromagnetic fields coupling to them and destroying the junctions. For research applications, one means of obtaining fast recovery is to make a coaxial array of very fast recovery diodes and to put them all around the thyatron.

Even if everything is matched a shunt inductor  $L_S$  not equal to zero is included in the system. When the load is a laser and it turns off with some voltage across it, some current has been flowing through  $L_S$  at that point. A voltage reversal may result, depending upon the ratio of the stored energies in the PFN and the shunt inductance (Fig. 18). Unfortunately,  $L_S$ , the inductance across the load, is usually fairly large to

FIGURE 17: INVERSE VOLTAGE REMOVAL DURING LOAD FAULTS



Now the "inverse diode" conducts during fault-induced voltage reversal on PFN, removing PFN voltage to zero before resonant recharging begins. If  $R_D = Z_N = R_D'$ , all voltage,  $V_{N-1}$ , is removed in the first reversal pulse.

NOTE: Even for  $Z_L = Z_N$ , for  $L_S \neq 0$  there is some current flow in  $L_S$ , thus at end of pulse:

$$i_{L_S} = \frac{V_L}{L_S}$$

$$\int_0^T V_L = - \int_0^T L_S \frac{di}{dt}$$

$$V_L \Delta T \approx L_S \Delta I$$

$$= L_S i_{L_S}$$

Can show:  $\frac{V_{N-1}}{L_N} \approx - \sqrt{\frac{L_{PFN}}{L_S}}$  and  $\Delta T = \tau$

$\therefore$  may need  $D_2$  even if  $Z_L = Z_N$



FIGURE 18: INVERSE VOLTAGE CALCULATION AND REMOVAL DURING LOAD FAULTS

At end of pulse of length  $\tau$ , for laser or magnetron loads, the load open circuits when the voltage is below the holding voltage (Sustaining Voltage)  $V_S$ . Energy stored in  $L_S$  charges  $C_N$  capacitance in PFN:

$$\therefore \frac{1}{2} L_S (i_{L_S})^2 = \frac{V_L^2 \tau^2}{2 L_S} \quad i_{L_S} = \frac{V_L \tau}{L_S}$$

And  $= \frac{1}{2} C_N V_{N-1}^2$

But Since  $Z_N = Z_L$   $V_L = \frac{V_N}{2}$

$$\therefore \frac{1}{2} C_N V_{N-1}^2 = \frac{1}{8} C_N V_N^2 = V_N^2 = \frac{V_N^2 \tau^2}{8 L_S}$$

$$\left( \frac{V_{N-1}}{V_N} \right)^2 = \frac{\tau^2}{4 L_S C_N}$$

But  $\frac{1}{2} C_N V_N^2 = \frac{V_L^2 \tau}{Z_L}$   $V_L = \frac{V_N}{2}$  &  $Z_L = Z_N$

$$\therefore \frac{1}{2} C_N V_N^2 = \frac{V_N^2 \tau}{4 Z_L} \quad Z_L = \sqrt{L_N / C_N}$$

$$\tau = 2 C_N Z_L = 2 C_N \sqrt{L_N / C_N} = 2 \sqrt{L_N C_N}$$

$$\therefore \left( \frac{V_{N-1}}{V_N} \right)^2 = \frac{1}{4} \times \frac{4 L_N C_N}{L_S C_N}$$

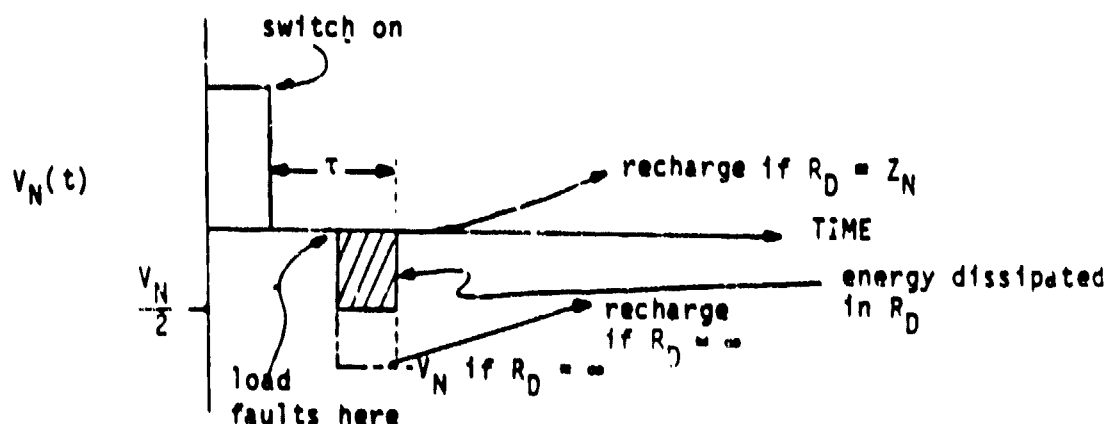
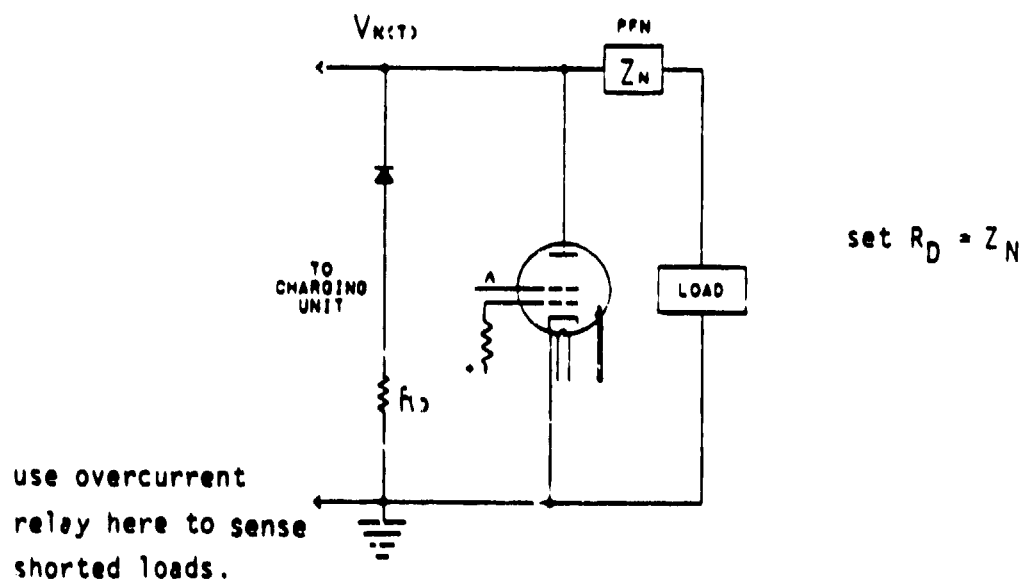
Or  $\left( \frac{V_{N-1}}{V_N} \right) = \pm \sqrt{\frac{L_N C_N}{L_S C_N}} = \pm \sqrt{\frac{L_N}{L_S}}$

WHERE THE SIGN DEPENDS UPON CURRENT FLOW DIRECTION: e.g., If  $I_{L_S}$  is the same sign  $I_L$  was, then negative sign is used since  $V_{N-1} \propto \frac{dI_L}{dt} < 0$ .

FIGURE 19: LOAD SHORT-CIRCUIT FAULTS

As we showed in Fig. 15, faulting in the load during discharge can dramatically increase the voltage the PFN is charged to in the following recharge. Only by providing an impedance-matched inverse diode network can this be avoided under all conditions. With present solid-state diodes and hydrogen diodes such a low impedance inverse network is almost always possible.

This network can also be connected across the PFN called an "end-of-line clipper" and serves primarily to clamp the PFN voltage reversal to low value and protect PFN capacitors.



keep the efficiency high; thus, even though the system has perfect matching there may be some need for inverse diodes to protect the tube from load faults.

The resistor  $R_D$  is normally quite a large value (several hundreds of ohms) and it is chosen to be large enough to keep the voltage across the switch tube negative until recovery is assured. For small tubes that can be 2  $\mu$ s, for larger tubes it can be 50 to 250  $\mu$ s.

#### X. EFFECTS OF LOAD SHORT CIRCUITS

Faulting in the load during discharge (Fig. 19) can dramatically increase the voltage to which the PFN is charged in the following recharge. Only by providing an impedance-matched, inverse-diode network can this be avoided under all conditions. With present solid-state diodes and hydrogen diodes, such a low-impedance inverse network is almost always possible. These comments pertain specifically to very long-lifetime systems (5 to 10 years) at kilohertz repetition rates with no component failure desired.

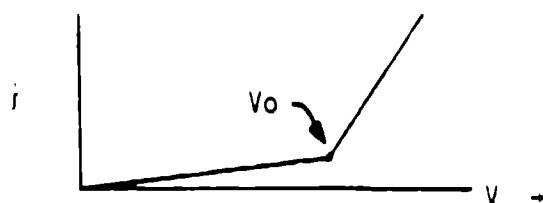
The network, consisting of a diode and a resistor, can also be connected across the PFN. When it is, it is called an end-of-line clipper and serves primarily to clamp the PFN voltage reversal to a low value and protect the PFN capacitors. When the load shorts there is a negative-going pulse, and the energy represented by the hatched area under the curve is deposited in  $R_D = Z_N$ , and recharge then occurs.  $R_D$  should be slightly smaller than  $Z_N$  so that sufficient negative voltage recovery time is available.

Note that the switch still must hold off  $V_N/2$  during the remainder of the discharge time (Fig. 20). Normally, restrikes of the switch will occur infrequently during these conditions. Adding an end-of-line clipper reduces the voltage by another factor of 2, clamping the PFN reversal to

FIGURE 20: INVERSE VOLTAGE APPEARING DURING LOAD FAULTS AND NONLINEAR CIRCUITS TO CONTROL THIS VOLTAGE

NOTE: The switch still must hold off  $\approx V_N/2$  during the remainder of the time  $\tau$ . Normally restrikes of the switch occur infrequently during these conditions. Adding an "end-of-line clipper" reduces the voltage by another factor of 2, clamping the PFN reversal to  $\approx V_{dc}/2$ . With fast circuitry they are "often replaced" and an inverse diode network only is used.

NOTE: True tetrode thyratrons are highly damage resistant to inverse internal arcing. They should be used whenever possible.



NONLINEAR CIRCUITS: The "mov" and "thyrite" materials have  $I \propto (V - V_o)^6$  so that they can replace all or a portion of  $R_D$  to reduce diode  $\frac{di}{dt}$  and allow larger peak currents:

$$\frac{di}{dt} < 3 \frac{KA}{\mu s} \quad (\text{Westinghouse 20 A stacks})$$

$$< 1 \frac{KA}{\mu s} \quad (\text{Westinghouse 5 A stacks})$$

-CONSULT MFR FOR PEAK CURRENT LIMITATIONS: Generally  $I_{pk}^2 t$  energy limit

less than  $V_{dc}/2$ . With fast circuitry, they fail rather frequently and an inverse diode network only is used.

What is normally meant by tetrode thyratrons is an anode, a control grid, a cathode structure, and an envelope with some hydrogen inside. Normally, there is a tiny pin stuck in the side of the grid structure, when forward biased, will reduce the jitter. That is not a tetrode tube; that is a tube that has a preionizer electrode in it. This tube otherwise behaves like an ordinary triode thyatron. A true tetrode thyatron actually contains another grid. An electron cloud is generated through forward biasing this first grid, and the potential well from the reverse-biased upper grid prevents these electrons from seeing the accelerating anode potential. Note that true tetrode (with two grids) thyratrons are highly damage resistant to inverse internal arcing. They should be used whenever possible.

In a large reliable system, fault current should be controlled with an inverse network. Current could be put through a time-varying resistor to keep the inverse voltage initially low and gradually discharge the PFN, reducing premature failure. This can be done with thyrite varistors. They are highly capacitive and difficult to use in kilohertz repetition-rate circuits.

The metal-oxide varistor and thyrite materials have  $I \propto (V - V_0)^6$ , ( $V_0$  is the turn-on voltage and  $V$  the applied voltage) so that they can replace all or a portion of  $R_D$  to reduce  $di/dt$  and still allow larger peak currents. Keeping  $di/dt$  less than 3 kA/ $\mu$ s for 20-A stacks and about 1 kA/ $\mu$ s for 5-A diode stacks is recommended by Westinghouse.

## XI. OPEN-CIRCUIT PROTECTION WITH CABLE INTERCONNECTIONS

Referring to Fig. 21, if the load is shorted, a wave is sent back and is multiplied repeatedly until the cable breaks down. If L and R are correctly chosen, the voltage pulse can be reduced significantly. In large systems with very high voltages there is no choice but to do this. In single-shot systems, a single point-plane spark gap connected to ground through a copper sulphate resistor is used to offer additional protection. If the laser faults, it sends back a -V and the point-to-plane gap across the cable input breaks down controlling this voltage. Such spark gaps can be used for high repetition rate systems, but erosion and gas flow needs may pose problems. In another circuit, the switch can be self-triggered. If relatively long pulses are used, a triggered spark gap protector can be added. When the wave comes back, a capacitive divider reduces the voltage and, fed through a diode, triggers the spark gap.

For cable connections to the load, either a shunt spark gap to ground or a shunt L/R network at each end of the cable is suggested to protect from overvoltages.

Figure 22 is a useful compilation of information on inductive loads prepared by Bill Nunnally.

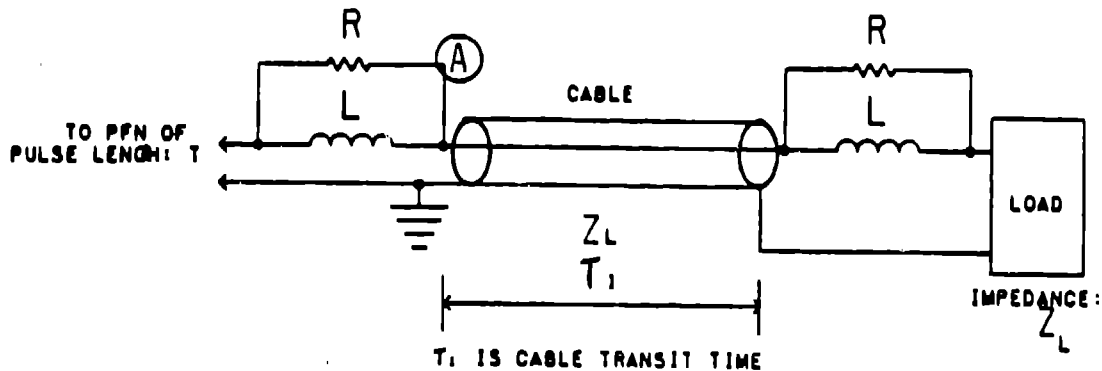
## XII. LASER LOADS

A. Direct-Discharge Pumped Excimer Laser Loads

Rare-gas halogen lasers, of considerable interest as sources of intense ultraviolet energy, represent one of the most challenging time-varying loads to come into existence in the last decade (Fig. 23). One of the difficulties in these systems is their time-varying nature.

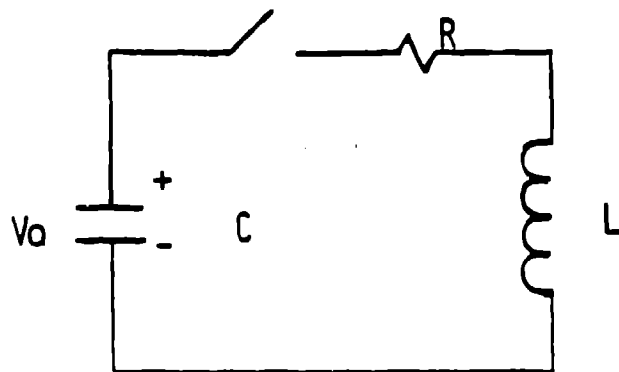
FIGURE 21: OPEN-CIRCUIT PROTECTION WITH CABLE INTERCONNECTIONS

For cable connections to the load, use a shunt spark gap to ground or a shunt L/R network at each end of cable to protect from overvoltages.

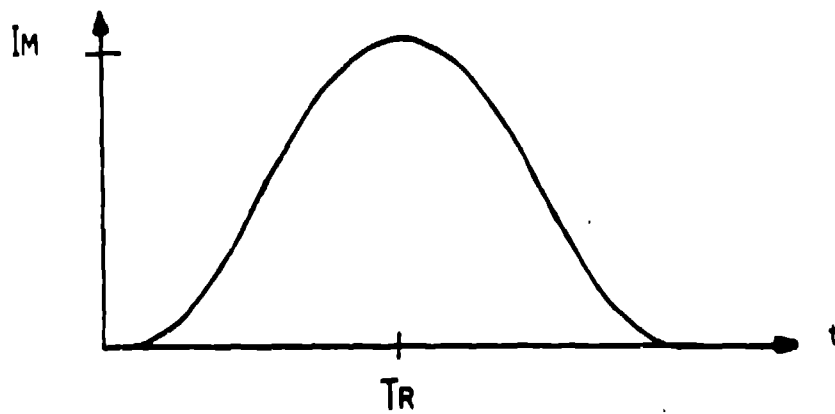


$L/R < \tau_R$  AND  $L/R \gg 2\tau_1$  for proper damping. If  $L/R = 2\tau_1$  then at time  $t = 2\tau_1$  voltage at (A) is  $\alpha(e^{-L/R \cdot t})V_N/2$   
 For load shorted:  $V_A = V_N/2 \times \{1/e^2\}$  (i.e., 90% damping) pick  $Q = \frac{\omega L}{R} = 0.5$   
 to quench oscillations; therefore voltage stress at (A) has been reduced from  $\approx 2 V_N$  to  $.05 V_N$  and only small oscillations are allowed.

FIGURE 22: CIRCUIT INFORMATION FOR INDUCTIVE LOADS



$$\frac{R}{2L} \ll \left( \frac{1}{LC} \right)^{1/2}$$



$$I_M = \frac{V_0 \pi C}{2 T_R}$$

$$V_0 = \frac{\pi L I_M}{2 T_R}$$

$$V_0 = \frac{I_M 2 T_R}{\pi C}$$

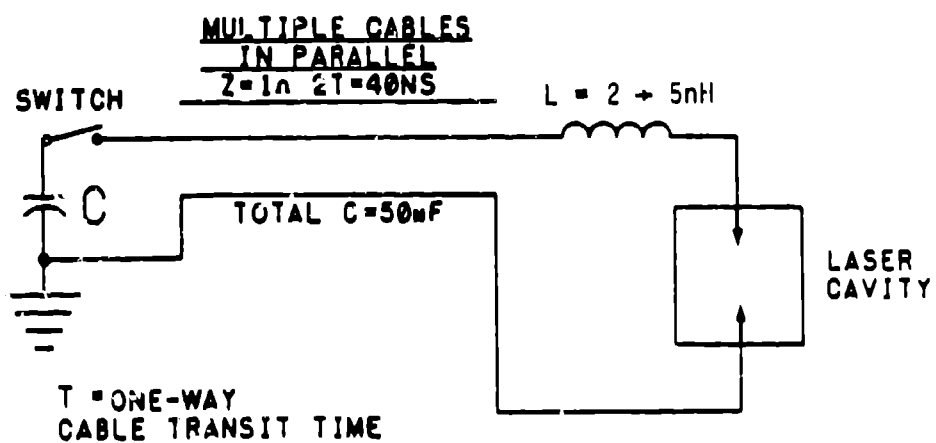
$$T_R = \frac{V_0 \pi C}{2 I_M}$$

$$C = \frac{2 T_R I_M}{V_0 \pi}$$

$$L = \frac{2 V_0 T_R}{\pi I_M}$$

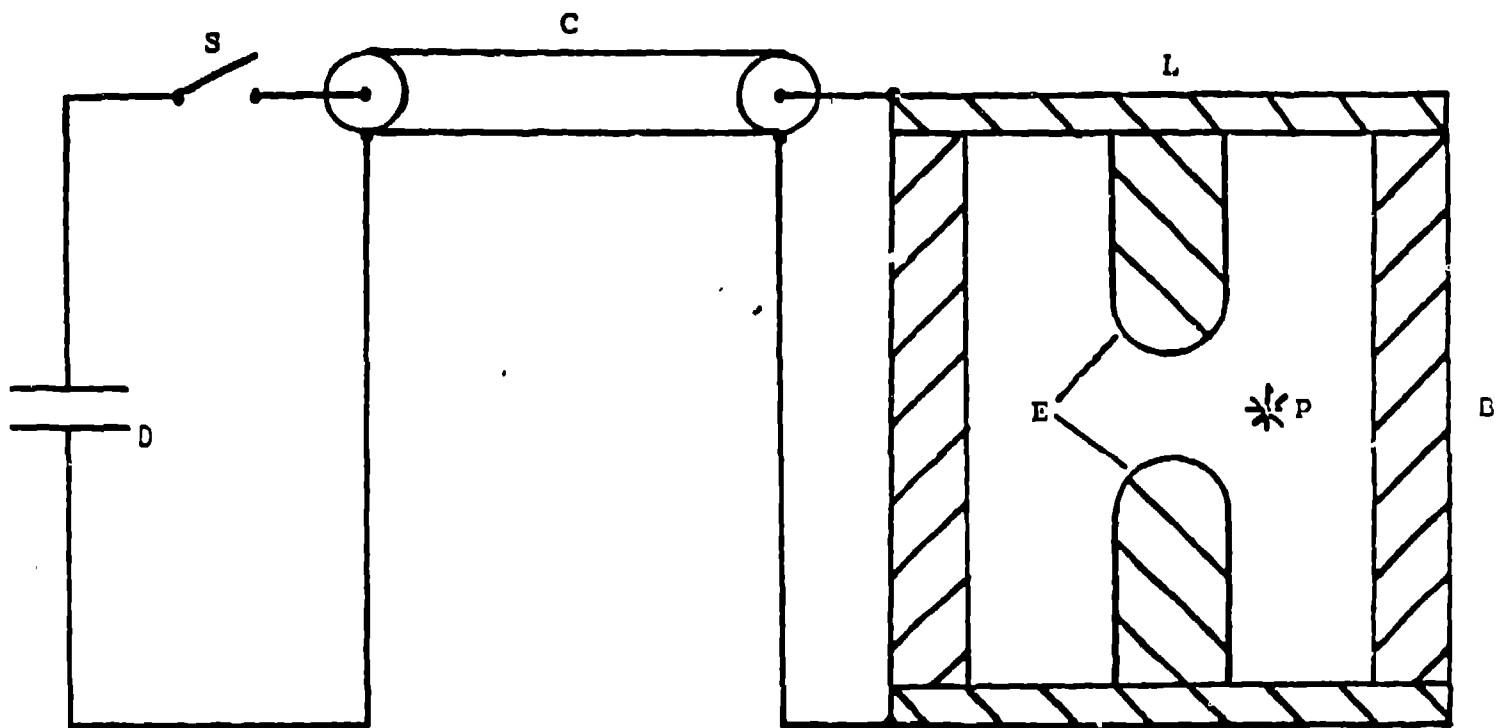


FIGURE 23: SIMPLIFIED EXCIMER LASER DRIVER



It is not unusual to see them go from many ohms to milliohms, making the maintenance of a constant  $V_L$  (which determines the excitation efficiency of the system) extremely difficult. Unlike the carbon dioxide laser, these discharge-pumped systems are quite unstable plasmas, so that the impedance of the krypton (or argon, xenon, etc.) helium, and fluorine mixtures decreases monotonically with time. These notes highlight the most extensive engineering study performed to date on the electrical characteristics of these lasers,<sup>9</sup> and time permits sketching only some of the interesting properties of these loads. Figure 24 schematically illustrates the type of Excimer laser of interest here. Energy is stored in the driver capacitor D and transferred into the cable capacitance C during and after the closure of the spark gap or thyatron switch S. The cable PFN generally has an impedance of 0.5 to 1  $\Omega$  and a discharge time approximately equal to the sum of the cavity time to break down plus the time to termination of the laser pulse. (This is close to the time the current takes to decay through zero.) As the switch closes, there is a permissible build-up time. Initially, the gas mixture is preionized by one of several means, here by an array of sparks P along the electrodes E. After a short delay, the switch S is closed and the voltage on the electrodes builds up from zero to breakdown in about 80 ns. Then a large current flows through the low-inductance load (L is approximately 2 nH). The most significant problem in this system is the rapid decrease in the load impedance with time, clearly indicating that conventional PFN design techniques are inappropriate to achieve the theoretically high efficiencies. To date, efficiencies in excess of 1% have been achieved at energies of  $\approx 1$  J. The major difficulty with this system is that when the switch closes it does so with a time constant, so the voltage on the electrodes has some build-up profile, either inductance limited or switch-resistive phase limited. Another major difficulty here is the current unavailability of lumped elements with parasitic inductances sufficiently low to allow the synthesis of time-varying PFNs required in this application. Devising techniques to effect such networks or transmission lines, whatever may be the highest pumping efficiency drivers for these systems, remains one of the more difficult power conditioning engineering problems today.

FIGURE 24: TYPICAL EXCIMER LASER



Typical Excimer Laser. D- driver capacitor; S- switch; C- cable  
PFN; L- aluminum plate; E- electrodes; P- preionization source;  
B- rigid dielectric body

Ref. 9

In these systems, the closure times of switches currently available are around 20 ns, significantly affecting the build-up times on the cavity electrodes and adding to the energy losses in the discharge loop. Advances in pulse-charged, very low inductance thyratrons and spark gap switches may well make long-life lasers of this class a reality. The remaining challenge will be to design and construct low-inductance, inverse-diode systems to protect the thyatron switches under conditions of laser cavity arcing.

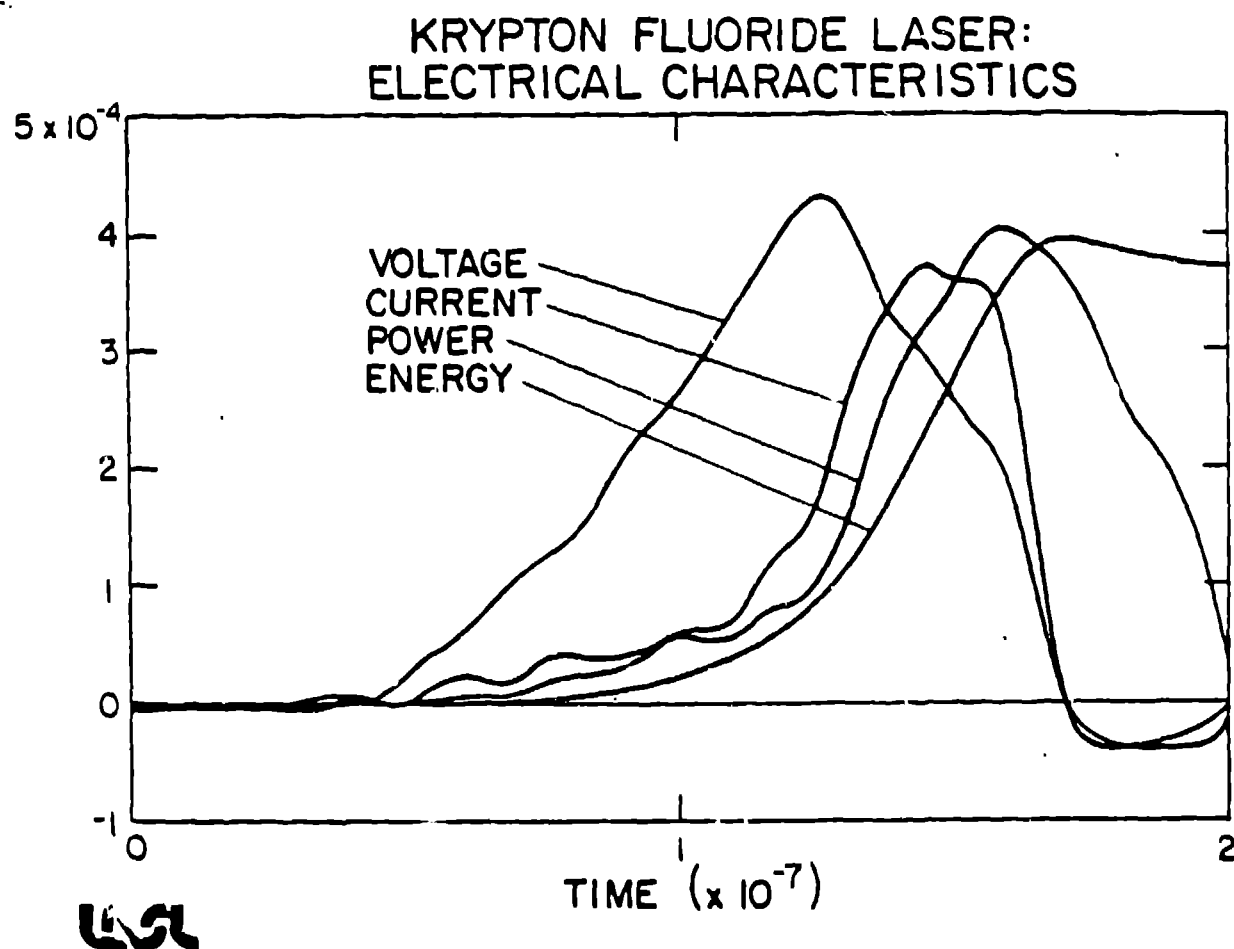
Figure 25 shows that for a KrF laser there is a voltage build-up until the discharge turns on. The current builds up to peak value while the voltage is decreasing. This is undesirable because the voltage must stay above a threshold level for optimal excitation kinetics. This threshold level is, unfortunately, rather high. Most of the energy deposited in the system is inefficient in pumping the laser. Ideally, a time-varying PFN is needed that has the reciprocal of the impedance of the discharge with time down to levels of  $\approx 50 \text{ m}\Omega$ . In contrast to this, typical extended-foil capacitors have an internal resistance of  $\approx 25 \text{ m}\Omega$ .

Figure 26 also shows the predicted power vs time and the predicted impedance vs time.<sup>9</sup> The agreement with the model is quite good.

#### B. Flashlamp Loads

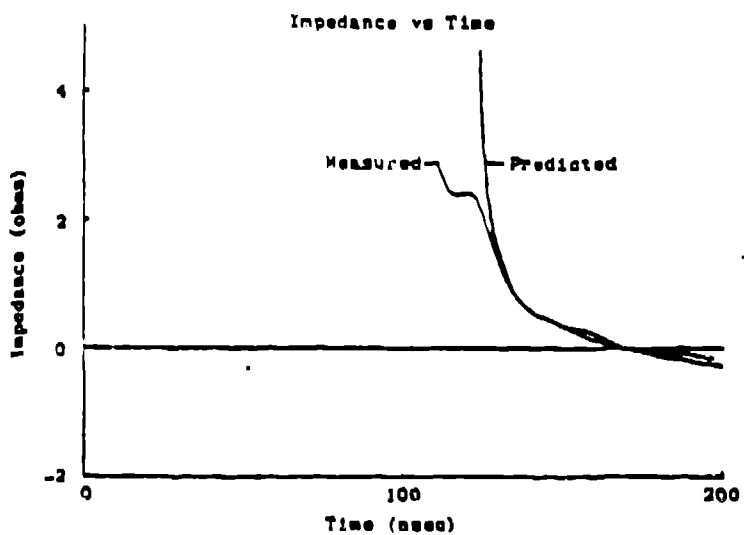
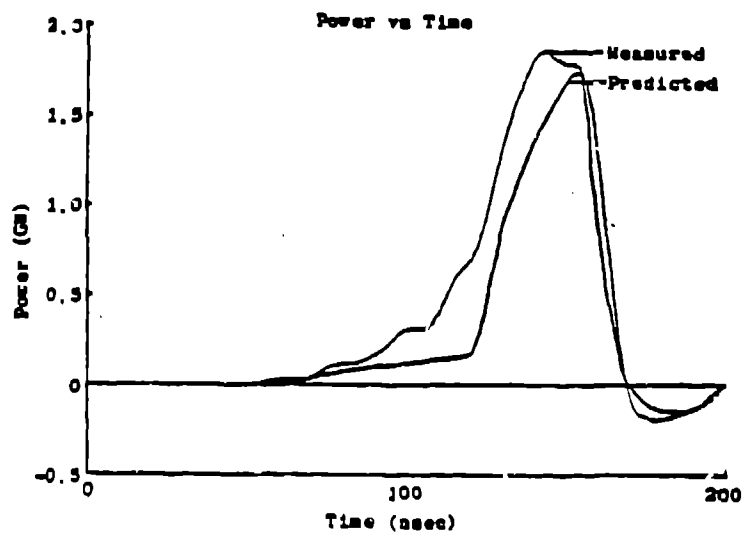
A flashlamp is a glass tube with two electrodes, containing xenon, krypton, or some other gas mixture at rather low pressures (Fig. 27). Assume a length  $l$  and a diameter  $d$ . Normal flashlamps are driven by long (multimicrosecond) pulses; there is very little concern about switch losses and they can even be driven with silicon-controlled rectifiers. Empirically, it has been shown that the lamp voltage is some constant times the square root of the current through it.<sup>10</sup>

FIGURE 25: TIME HISTORY OF CIRCUIT AND SYSTEM PARAMETERS IN THE DISCHARGE-PUMPED KrF\* LASER



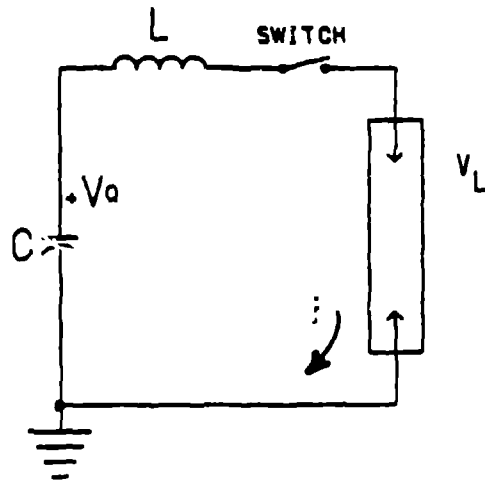
Ref. 9

FIGURE 26: COMPARISON OF PREDICTED AND MEASURED POWERS AND IMPEDANCES IN THE DISCHARGE-PUMPED KrF\* LASER



Ref. 9

FIGURE 27: FLASHLAMP LOADS



FLASHLAMP: of length  $l$  cm  
diameter  $d$  cm

Containing Xenon or Krypton

Pulse widths are typically 5 to 125  $\mu$ s so that switch losses can be neglected.

$$V_L = \pm k/i^{1/2}: \text{ Empirically determined}$$

For small voltage reversals on C and maximum energy transfer into the lamp in the first current  $\frac{1}{2}$  cycle: (say = 20% reversal as determined by the cost for C for a given lifetime)

- Then:
1.  $K = 1.3 \frac{1}{d} \left( \frac{P}{P_1} \right)^2$   $P_1 = 450$  torr for xenon  
 $P$  = Actual xenon pressure in flashlamp
  2.  $U = \frac{1}{2} C V_0^2$ : Energy stored in capacitor.
  3. Let  $\tau$  = Pulse width (not FWHM but zero to zero of current).  
 $\tau = \pi \sqrt{LC}$
  4.  $C^3 \approx \frac{0.5}{9} \frac{U \tau^2}{K^4} \approx \frac{0.05 U \tau^2}{K^4}$
  5. Check U explosion =  $6.8 \times 10^4 l d (LC)^{1/2}$ . 50% probability of explosion  
( $\tau > 10 \mu$ s) =  $3.8 l d \sqrt{\tau}$

Ref. 10

Capacitor cost can be reduced by allowing a small, say 20%, reversal and designing for maximum energy transfer in the first current half cycle. If the light output of the lamp and the energy to be deposited in the lamp are known, the explosion limits for relatively long pulses can be determined. When the energy stored in the capacitor is equal to the determined energy, there is a 50% chance that the lamp will blow up. In most circuits, it has been found that the longer lamps can be operated near the explosion limit.<sup>10</sup>

The most convenient way to trigger a flashlamp is with a series injection trigger transformer, usually on the ground end. This generates a pulse that exceeds the self-break voltage of the lamp and the lamp turns on. The fluctuations in the breakdown time can be significantly reduced by overvolting the lamp by a factor of 2.

#### C. Carbon Dioxide Laser Load

There are two kinds of CO<sub>2</sub> lasers: electron beam lasers and TEA lasers. The latter are similar to the Excimer laser, wherein their impedance decreases with time, but at a slower rate. The CO<sub>2</sub> lasers with electron-beam-controlled discharge systems, for example, basically act as resistive loads with some turn-on voltage. The gas discharge voltage can be provided by a Marx bank. If the pumping voltage wave form is altered to rise more quickly the gain rises faster, permitting more energy to flow out of the system for shorter optical pulses into it. Experimenters have looked into a type C PFN, with two sections (two L and C, one each per section in the PFN) and have derived the voltage pulse shown in Fig. 28. This worked very well.<sup>11</sup>



FIGURE 28: CARBON DIOXIDE LASER LOADS

## Electron beam controlled discharge

- pure resistive load compared to diode magnetron type of load
- can use type C PFN in Marx stages
- large units:  $Z = 3 \Omega$  for  $2.5 \mu s$  discharge times

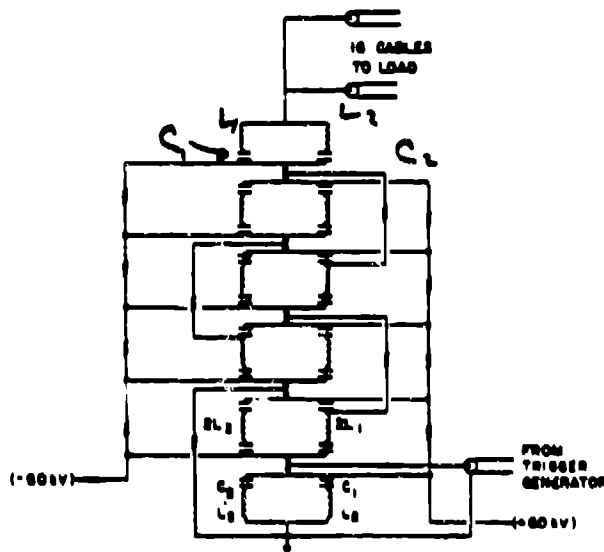


FIG. 1. 600-kV, 2.5- $\Omega$  type-C Guillemin-Marx network. This is the ideal circuit ignoring stray inductance. Circuit element values are discussed in the text. A "stage" is considered to be a spark gap, a set of positively charged capacitors, and a set of negatively charged capacitors.

## PER STAGE: TYPE C PFN

$$L_1 = 0.63 C_1 Z_0^2$$

$$L_2 = 6.5 C_2 Z_0^2$$

$$C_1 = 0.40 \frac{T}{Z_0}$$

$$C_2 = 0.042 \frac{T}{Z_0}$$

Defining  $\tau$ ,  $V_{pk}$  and  $U$  stored defines all the particular components.

then  $C_1 = 8.6 F$

$C_2 = 0.58 F$  For

$L_1 = 220 F \quad Z_0 = 2.5 \Omega$

$L_2 = 235 F$

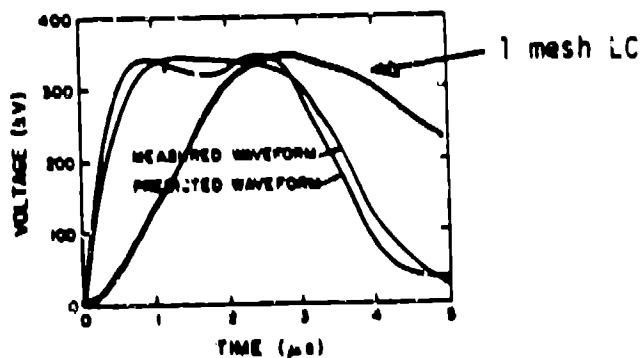


FIG. 3. Predicted and actual waveforms into a 3- $\Omega$  dummy load in the PFN unit.

## Advantages for Resistive Load:

1.  $V_{pk}$  per stage times  $n = V_L$
2. Stray  $L$  in connection loop affects risetime but not peak power.
3. Waveform readily changed.  
∴ Can use with time varying loads.

The TEA lasers are like HF and KrF lasers that are discharge pumped. They can be made to work very well at high-repetition rates, but everything that has been said about the KrF laser can be said about TEA lasers, multiplying the time-scale of excitation by a factor of 10. The TEA lasers also have a smaller decrease in impedance with time, compared to KrF lasers the ratio is considerably less.

#### D. Discharge-Pumped Hydrogen Fluoride Laser Load

The HF lasers are attachment-dominated and the impedance decreases with time (Figs. 29 and 30). Impedance was measured as a function of current in kiloamps for different pressures of the gas (Fig. 31). To design this particular system, one must choose a pulse width less than the arcing pulse duration ( $\approx 0.25 \mu\text{s}$ ). Even if the electric field is kept constant, the gas heats with time until it experiences thermal breakdown. This is a common characteristic power-loading limit of all lasers.

#### XIII. SUMMARY

Generally speaking, with the exception of electron-beam systems, lasers all have decreasing impedances with time. This presents a challenging area for research to provide high-efficiency lasers with electrical PCS drivers optimized to meet the load excitation kinetics requirements.

FIGURE 29: DISCHARGE-PUMPED HYDROGEN FLUORIDE LASER LOAD

1. Electrical drive similar to KrF\* laser discussed before.
2. From experiment: Impedance decreases with increasing discharge current: A time-varying load.

- Take  $Z$  at peak current to design PFN with peak voltage determined from a scaling experiment.
- Design PFN width for optimum pumping and pulse termination before the onset of arcing ( $\approx 300$  ns for a laser electrode spacing of 5 cm)

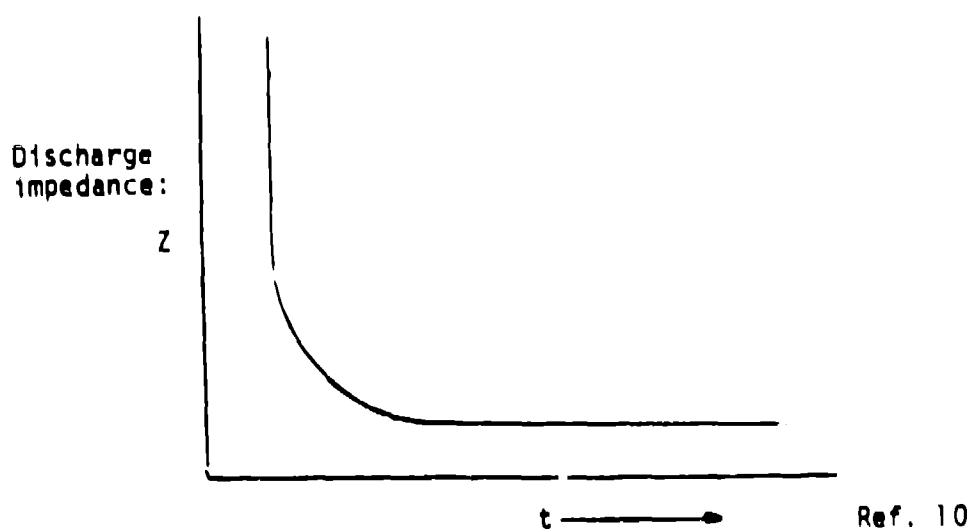
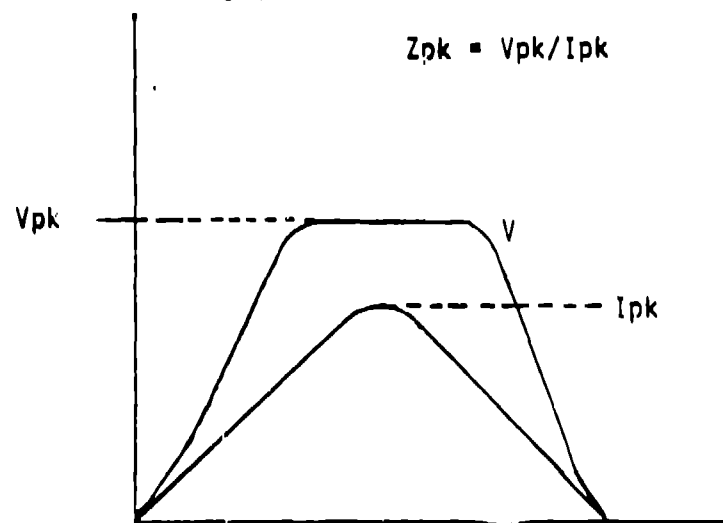


FIGURE 30: DISCHARGE-PUMPED HYDROGEN FLUORIDE LASER LOAD

## 3. Results of the calculations

-Used NET 2 program and incorporated  $L$  of each capacitor as part of the PFN. Type E-C hybrid PFN could be designed analytically but far more cost effective to use computer.

## 4. Short circuit ringing tests:

- a. short cavity
- b. from ringing following may be determined

$$I_{pk} \propto I_0 e^{-R/L \cdot t}$$

$$\therefore \ln I_{pk}^+ = \ln I_0 - \frac{R}{L} \tau/4$$

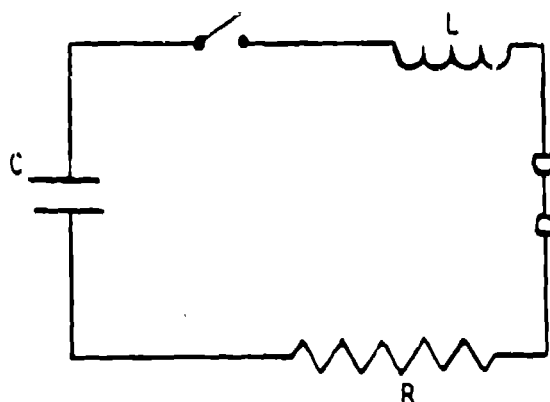
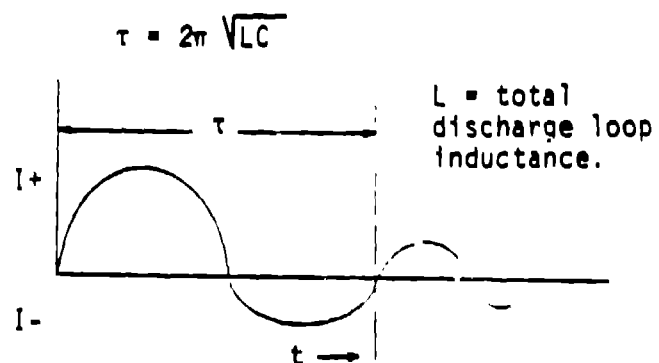
$$\ln I_{pk}^- = \ln I_0 - \frac{R}{L} 3\tau/4$$

Subtract

$$\ln I_{pk}^- - \ln I_{pk}^+ = \ln (I_{pk}^- / I_{pk}^+) = \frac{R}{4L} \cdot (3-1) \tau = R\tau/2L$$

$$= \frac{R}{2L} \cdot 2\pi\sqrt{LC} = \pi R \sqrt{C/L} = \ln (\text{Damping ratio})$$

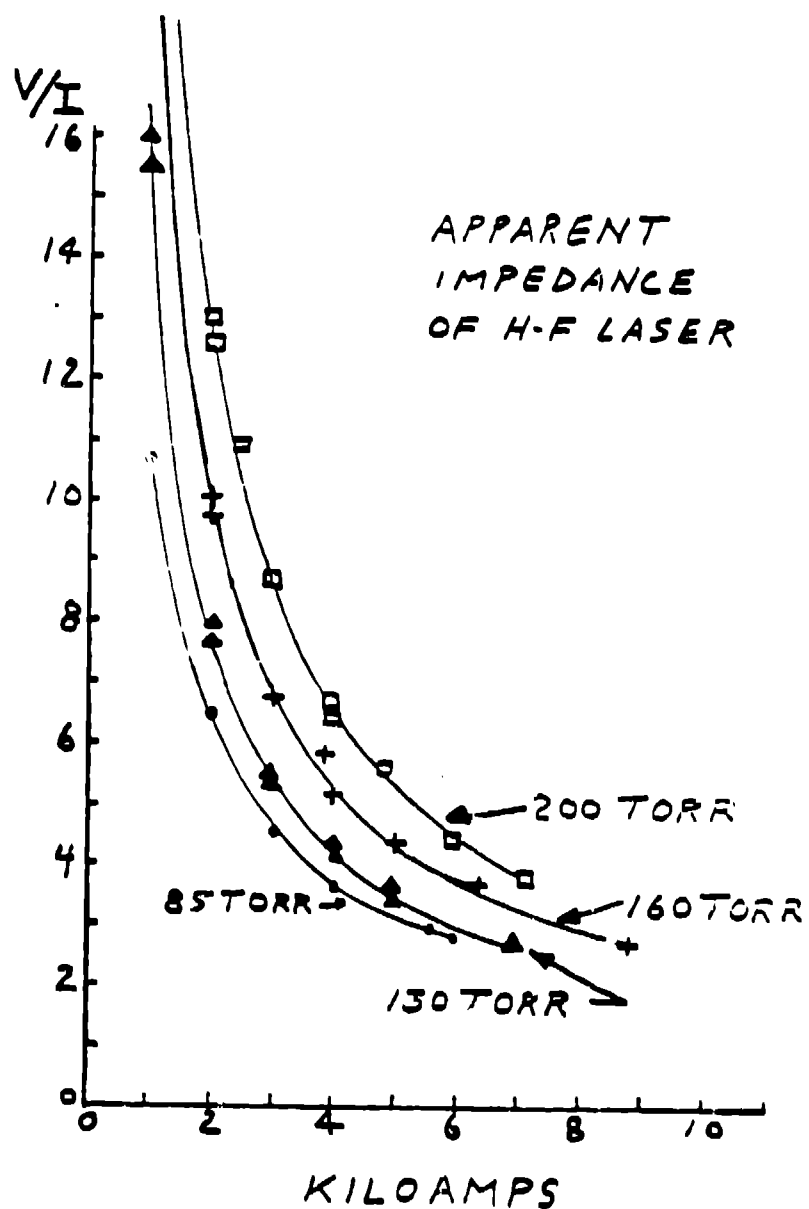
$\therefore$  obtain "L" and "R"



SHORT CIRCUIT LASER CAVITY  
RINGING EXPERIMENT

Ref. 10

FIGURE 31: APPARENT IMPEDANCE OF THE DISCHARGE-PUMPED HYDROGEN FLUORIDE LASER LOAD



## REFERENCES

1. G. N. Glasoe and J. V. Lebacqz, Pulse Generators (McGraw-Hill, New York, 1948).
2. W. J. Sarjeant, "Energy Storage Capacitors," LASL Report No. LA-UR-79-1044, August 1979. (See also Lecture 4, Appendix of EECS596 "High Voltage/Pulse Power Technology," UNM graduate course).
3. T. P. Sorensen and V. M. Ristic "Risetime and Time-Dependent Spark-Gap Resistance in Nitrogen and Helium," Journal of Applied Physics, Vol. 48, No. 1, January 1977, pp. 114-117.
4. W. L. Willis, "Spark Gaps," Los Alamos Scientific Laboratory Report No. LA-UR-80-634, (see also Lecture 6 of EECS596 "High Voltage/Pulse Power Technology," UNM graduate course).
5. W. J. Sarjeant and W. C. Nunnally "A Kiloherzt Trigger System for Multichanneling a 100-kV Mid-plane Spark Gap," Los Alamos Scientific Laboratory Memorandum No. E-4-79-101, March 5, 1979.
6. A. E. Greenwood, Electrical Transients in Power Systems, Wiley-Interscience, New York, 1971).
7. G. Metzger and J. P. Vabre, Transmission Lines with Pulse Excitation, (Academic Press, New York, 1969).
8. "Hydrogen Thyatrons -- Theory and Applications," General Electric Technical Literature.
9. R. R. Butcher, "A Comprehensive Study of Excimer Laser Systems," Los Alamos Scientific Laboratory thesis report LA-7329-T, June 1978.
10. W. L. Willis, unpublished data.
11. K. B. Riepe, "High-Voltage Microsecond Pulse-forming Network," Rev. Science Instrumentation, Vol. 48, No. 8, August 1977, pp. 1028-1029.